NASA Technical Memorandum 78735

Effluent Monitoring of the December 10, 1974, Titan III-E Launch at Air Force Eastern Test Range, Florida

Dewey E. Wornom and David C. Woods
Langley Research Center
Hampton, Virginia

National Aeronautics
and Space Administration

Scientific and Technical Information Office

1978

SUMMARY

This report contains the experimental field measurements of the ground-cloud behavior and effluent dispersion from a Titan III-F rocket launched from the Air Force Eastern Test Range (Launch Complex 41) on December 10, 1974, at 0711 UT (0211 EST). The measurements were obtained as part of a continuing launch-vehicle-effluent monitoring program conducted jointly by the Langley Research Center, Marshall Space Flight Center, and Kennedy Space Center. The objective of the program is to obtain experimental field measurements in order to evaluate a model used to predict launch-vehicle environmental impact.

For this launch the ground cloud rose at 4 m/sec (the predicted average rate was 5 m/sec) and then broke up into at least two separate clouds after passing through a combined temperature inversion and wind shear layer at a 0.6-km altitude. One cloud rose past the predicted 0.82-km stabilization height and stabilized at 1.4 km, but did travel in the predicted southeasterly direction where surface instrumentation was deployed. Another cloud, sampled by a specially instrumented aircraft, stabilized around 0.07 km below the predicted 0.82-km altitude but traveled in a southerly direction.

Twenty penetrations of the southerly moving cloud were made by the sampling aircraft during the period 3 to 55 min after launch. Maximum measured effluent levels in the cloud were 45 ppm hydrogen chloride (HCl) and 371 $\mu g/m^3$ aluminum oxide (Al_2O_3). During the last pass maximum concentration of 25 ppm HCl was measured. No diffusion-model predictions are available for comparison with the in situ cloud measurements.

The highest level of surface HCl measurements obtained was 0.50 ppm 4 km from the launch pad. The remaining surface HCl measurements decreased with distance from the pad to a lowest value of 0.023 ppm at 11.5 km. The highest surface Al_2O_3 measurement of 1274 $\mu g/m^3$ was obtained on the launch pad. Other surface Al_2O_3 measurements varied from 168 to 1.2 $\mu g/m^3$ but were not consistent with distance from launch pad. Although direct comparison of measurements and model predictions revealed inconsistencies, overall results indicate that the model predictions were high. However, the highest surface measured level of 0.50 ppm HCl 4 km from the launch pad compares favorably with a predicted level of 0.56 ppm 5 km from the pad.

INTRODUCTION

The National Aeronautics and Space Administration is conducting studies to determine the environmental impact of firing solid rocket motor (SRM) launch vehicles. Part of these studies are directed toward validating a tropospheric diffusion model. Such models will be used to predict the impact of future rocket launches upon the quality of surrounding surface air and establish launch constraints if necessary. To assess the applicability and accuracy of such models, a Launch Vehicle Effluent (LVE) monitoring program of Titan III launch

vehicles is being conducted by the Langley Research Center (LaRC) at the Air Force Eastern Test Range (AFETR) in Florida. The resulting measurements are then compared with predictive output of the Marshall Space Flight Center (MSFC) diffusion model of reference 1. This report summarizes LVE measurements obtained during the Titan III-E (Helios A) launch from the AFETR Launch Complex 41 (LC-41) on December 10, 1974, at 0711 UT (0211 EST). Previous monitoring activities have been reported in references 2 to 6.

During lift-off, the SRM exhaust from launch vehicles forms into what is commonly referred to as the "ground cloud." Contained within the cloud, as noted in reference 7, are such effluents as hydrogen chloride (HCl), aluminum oxide (Al_2O_3), carbon monoxide (CO), and carbon dioxide (CO_2). These effluents are dispersed upon the ground as the buoyant cloud diffuses into the ambient air, rises to a stabilized altitude (dependent upon its heat content and local mixing-layer height), and drifts with the prevailing wind. The measurements presented herein consist of the cloud rise and subsequent stabilization height, direction of travel, in situ cloud effluent concentrations, and surface effluent concentrations. These actual field measurements are then compared with the predictive output of the MSFC multilayer diffusion model based on real-time measured meteorological conditions.

Use of trade names or names of manufacturers in this report does not constitute an official endorsement of such products or manufacturers, either expressed or implied, by the National Aeronautics and Space Administration.

The authors wish to acknowledge the cooperation and support of the Kennedy Space Center, MSFC, the U.S. Air Force, and their contractors during this experimental field measurement activity.

LIST OF ABBREVIATIONS

AFETR	Air Force Eastern Test Range
EST	eastern standard time
KSC	Kennedy Space Center
LaRC	Langley Research Center
LC-41	Launch Complex 41
LVE	launch-vehicle effluents
MSFC	Marshall Space Flight Center
NA	not applicable
NAA	neutron activation analysis
NASA	National Aeronautics and Space Administration
P	primary instrument site

ppm	parts per million (volume/volume)
QCM	quartz-crystal mass monitor
S	secondary instrument site
SRM	solid rocket motor
T	time relative to launch; T-0 is launch
TVC	thrust vector control
UCS	universal camera site
UT	universal time

PROGRAM DESCRIPTION

Launch Vehicle

The Titan III launch vehicle, shown at lift-off in figure 1, was developed by the U.S. Air Force for space launches at the eastern and western test ranges. The launch vehicle consists of a three-stage liquid propulsion core and two solid rocket motors (SRM) attached on opposite sides of the core. Since the staged liquid propulsion core is ignited at altitude, only the SRM and a thrust vector control (TVC) system contribute to the effluent composition in the ground cloud. Letter designations, such as III-C and III-E, refer only to the staged core, and thus do not alter the effluents within the ground cloud. The SRM propellant consists of an ammonium perchlorate oxidizer, an aluminized synthetic-rubber binder fuel, and various other additives to stabilize mass and control the burning rate. The major exhaust effluents from the SRM are HCl, Al_2O_3, and CO. The TVC constituents decompose in the SRM exhaust to nitric oxide (NO) and oxygen (O_2). Composition of the exhaust at the nozzle exit plane (ref. 8) and 1 km from the exit plane (ref. 9) is shown in table I.

Instrumentation

Optical tracking system.- Three optical tracking units (Askania cameras), as described in reference 10, were employed to record the rise and downwind track of the ground cloud as a function of time. Tracking was performed by camera operators visually sighting on the cloud centroid. Two searchlights were utilized to assist in the visual sighting during this nighttime launch. Cloud photographs, normally taken for cloud growth, were not possible due to insufficient lighting.

Surface sampling instrumentation.- The surface sampling instrumentation deployed for this launch is listed in table II. The primary sets are manned and contain continuous monitoring instruments which measure effluent concentrations. These primary sets are critically positioned relative to the predicted

path of the ground cloud and the predicted location of peak surface concentration. The remaining instrument sets are remotely activated and measure effluent dosage. The capabilities of the instruments are given in table III with more detailed information reported, as noted in the table, in references 5, 9, 11, and 12.

Airborne sampling instrumentation.- A light twin-engine aircraft was instrumented by NASA LaRC specifically for in situ sampling of the ground cloud at altitude. The LaRC aircraft was employed for the first time during this launch monitoring activity. The capabilities of the instruments aboard this aircraft are listed in table IV with complete details of the instrumented aircraft given in reference 13.

Deployment of Instrumentation

Cloud tracking system.- The three tracking camera locations - universal camera sites (UCS) 2, 9, and 26 - relative to LC-41 are shown in figure 2. These locations were selected such that the cloud would always be in the field of view of at least two cameras. Cloud centroid position was recorded by these cameras in 10-sec intervals after launch until the cloud was no longer visible or went out of view of a given camera.

Surface sampling instrumentation.- Prelaunch predictions of effluent diffusion and cloud trajectory, provided by MSFC, were used for positioning the surface sampling instrumentation. These predictions were generated by the diffusion model of reference 1 using meteorological data (summarized in ref. 14) from the USAF Air Weather Service at AFETR, local wind towers, and rawinsonde releases. Additional wind data, as shown in figure 3, were provided by tetroon flights 8 hr before and 85 min after launch. The predictions for this launch, from T-24 hr to T-3 hr, are presented in table V. The deployment and operational times for the instruments are given in table VI.

The locations of the surface sampling instruments are listed in table VII and shown in figure 4. The tower site was prepared 2 days prior to launch in the launch pad area. The fallback sites were selected based on the cloud prediction at T-24 hr of table V. From this prediction, a cloud trajectory of 158° from LC-41 would carry the ground cloud out to sea. To prepare for this possibility, seacraft were obtained as platforms for the surface sampling instruments. At T-9 hr, when final commitment of seacraft deployment must be made, the cloud trajectory was predicted to be about 150° but meteorology data indicated a probable southerly shift by launch time. Therefore, a combined land and sea deployment for the primary sites was initiated. Five seacraft (P-1 to P-5) were deployed based on the prediction at T-14 hr (147° cloud trajectory) with P-1 being located at the predicted HCl peak concentration point (6.6 km from LC-41) and the remaining seacraft (P-2 to P-5) located at other positions along the predicted cloud trajectory. (See fig. 4.) Due to a possible southerly shift in the cloud trajectory, the remaining primary sites (P-6 to P-9) were located along the coastline. Positioning of the five seacraft was accomplished through the use of a sixth seacraft equipped with a Lorac and radar system. At T-6 hr, when final commitment of the secondary instrumentation had to be made, the predicted cloud path had shifted more southerly to 185°. Thus,

the secondary instrument sites were located as shown in figure 4 based on the 185° trajectory and projected meteorology data which indicated that the launch-time trajectory would shift easterly from 185°. The prediction at T-3 hr in table V was used to update the sampling schedule for all instrument sites and provide cloud-path and stabilization-altitude data for both the optical-tracking and airborne-sampling personnel.

Airborne-sampling instrumentation.- The aircraft left Patrick Air Force Base, Florida, at T-1 hr and went into a race-track holding pattern at an altitude of approximately 1 km southwest of the KSC Vertical Assembly Building. At T-0 the aircraft was radar directed toward the launch pad by the radar vector controller to commence sampling the ground cloud. Aircraft basic sampling procedure is to make successive straight and level penetrations through the cloud centroid (based on pilot visual determination) alternately in a downwind then crosswind direction. (See fig. 5.) However, for this launch the first pass was made over the top of the cloud, through the base of the rocket exhaust plume, to obtain a measurement of plume effluent concentrations. Thereafter, attempts were made to perform alternate downwind and crosswind passes but these were not always executed successfully due to difficulty in maintaining visual contact with the ground cloud during this night-time launch. Speed of the aircraft during sampling was maintained at approximately 51 m/sec. Aircraft position data while sampling were obtained by the AFETR Mod II SCR-584 radar of reference 10. For passes 3 to 9 the aircraft passed near the radar location and the radar was unable to continue tracking due to limitations of its azimuth and elevation rate change.

Aircraft sampling parameters for each pass through the ground cloud are listed in table VIII. For this night launch two searchlights were directed at the ground cloud to assist the aircraft in making visual contact with the cloud. After the ninth pass the searchlights, and therefore the aircraft, lost contact with the cloud. At that time the aircraft returned to and crossed over the launch pad on an estimated cloud-intercept heading and altitude. However, visual contact was regained again only by lights from a populated area on the ground reflecting off the cloud.

RESULTS AND DISCUSSION

The data discussed herein are the cloud behavior (which included rise, stabilization height, and ground trajectory) and effluent measurements. Where applicable, postlaunch model predictive data are compared with the measured results. Predictive data for comparison with the airborne in situ sampling are not available.

Postlaunch Diffusion Model Predictions

Postlaunch model predictions based on launch-time meteorological conditions are provided by MSFC using the diffusion model of reference 1. The predicted cloud behavior is presented in tables IX and X. Predicted surface effluent levels, with respect to the deployed primary instrumentation site location, are given in table XI. Since the cloud broke up into at least two

separate clouds, the model predictions were based on the cloud closest to the ground (the one sampled by the aircraft). Additional predictive data are also presented in figure 6. The meteorology used for the predictions was comprised of rawinsonde and Jimsphere data (ref. 14) and is presented in figure 7.

Cloud Behavior

Cloud rise and stabilization.- Cloud rise and stabilization data are presented in figure 8. The error bars associated with the optical tracking measurements represent the uncertainty in the measurements as noted in reference 4. Although tracking continued to T+30 min, data beyond T+13 min are not presented since large measurement errors occurred due to poor nighttime visibility.

Figure 8 shows that the optically tracked cloud rose at a rate of approximately 4 m/sec and reached a stabilization altitude around 1.4 km at T+8 to 10 min. Comparatively, the model predicted a slightly higher average rise rate of approximately 5 m/sec. The aircraft sampling altitude for the passes shown (except pass 1 which was not attempted through the cloud centroid) indicates a cloud stabilization height of 0.75 km. Since the model predictions were based on the cloud sampled by the aircraft, the predicted stabilization height of 0.82 km should be compared to the aircraft sampling altitude of 0.75 km instead of the stabilized height of 1.4 km determined by the optical tracking system. The significant discrepancy in cloud-stabilization-altitude data, between the optical tracking and sampling aircraft, suggests that the cloud might have separated into several pieces each stabilizing at different altitudes. Unfortunately, no cloud photographic data were obtainable during the nighttime launch to assist in determining whether the cloud actually separated. Considering the combined wind-direction reversal and temperature inversion layer at 0.6 km, shown in figure 7, such a condition should have resulted in cloud breakup as it passed through this altitude. The wind-direction reversal persisted until at least T+14 min, as shown in figure 7, based on Jimsphere data from reference 14.

Cloud ground trajectory.- Cloud ground-trajectory data are presented in figure 9. The error bars associated with the optical tracking measurements represent uncertainties in the measurements as noted in reference 4. The comparison between the predicted southeasterly cloud trajectory and the southeasterly optically measured trajectory indicates reasonable agreement. Also, the predicted 8.3-m/sec rate of cloud movement compares favorably with the optically measured average value of 9.7 m/sec. However, it should be noted that the model predictions were not made with reference to the optically tracked cloud.

As with the stabilization height, the sampling aircraft position during its passes through the cloud is not in agreement with the optical tracking measurements. As seen in figure 9, the aircraft was sampling in a southerly direction as opposed to a southeasterly cloud movement recorded by optical tracking. That the aircraft monitored a cloud obviously in a different place from the one tracked optically substantiates the theory that the ground cloud did actually break up into at least two separate clouds.

Airborne Effluent Measurements

Continuous measurements of HCl and particles obtained during 20 aircraft passes through the ground cloud are presented in figure 10 as a function of time from launch. The HCl measurements were obtained by a chemiluminescent detector of reference 11. Two rapid-response instruments, an integrating nephelometer and a quartz-crystal mass monitor, described in reference 6 were used to measure particulate mass concentrations. In addition, mass concentrations of particles per pass collected on filters within a concentrator (ref. 13) are presented in table XII.

Hydrogen chloride.- Normally, the effluent concentrations within the ground cloud are expected to decrease with time as the cloud expands and dilutes. However, it is noted in figure 10 that between passes 9 and 10 the measured effluent levels increased. The measured HCl peak level, for example, gradually decreased from an initial level of 45 ppm for pass 2 (pass 1 was not attempted through the cloud centroid) to approximately 20 ppm for pass 9 and then increased to about 30 ppm for pass 10 before continuing to decrease again. The same phenomenon also occurred in the case of the particle measurements. Sufficient data are not available to understand these unexpected results. It is known that the ground cloud, after passing through an altitude of 0.6 km, separated into at least two clouds. It is also known that after pass 9 the aircraft did not regain visual contact with a cloud until 11 min later. Whether the relocated cloud was the initially sampled cloud or some other source from the launch vehicle cannot be determined with the data available.

Particles.- The integrating nephelometer measures the scattering coefficient of the suspended particles and the mass concentrations presented in figure 10 are inferred through an empirical relation established from limited data of reference 15. Since the response of the instrument depends on the amount of light scattered by the suspended particles it is influenced by particle size distribution and their refractive index as well as the mass concentration. The response also depends on the combination of these factors. It has been demonstrated that for various combinations of refractive indexes and size distributions uncertainties in the estimated mass concentrations may be in error by as much as a factor of 4. (See ref. 16.) It should therefore be recognized that while the nephelometer was used primarily because of its rapid time response (2 to 3 sec as installed) and its ability to determine the profile of the ground cloud, the inferred mass concentrations may be in large error.

Since the quartz-crystal mass monitor (QCM) measures mass directly, its response does not depend on particle size distribution nor refractive index. Therefore, the large errors in mass concentration caused by these factors in the integrating nephelometer are not present with this instrument. There were, however, problems associated with high relative humidity and hygroscopic particles which caused abnormal responses in the instrument. In many cases the hygroscopic particles would impact on the crystal then absorb moisture from the incoming sampling air. This would cause a response corresponding to a high mass concentration. A short time later the moisture would evaporate resulting in a loss of mass from the crystal surface. The instrument would respond rapidly in the negative direction indicating an apparent negative mass concentration. This type of response is illustrated in pass 2 of figure 10. In this

case the QCM trace is not consistent with the nephelometer trace. Evaporation of moisture is indicated by the negative swing and absorption by the positive overscaling. When this happens there is no way of extracting the correct mass concentration from the trace and the data are useless. This problem occurred for all passes through the cloud except for passes 1, 6, and 7. In each of these cases a fresh unexposed crystal which had no deposit of hygroscopic material on the surface was employed. Therefore, since there were no particles on the crystal surface initially to absorb moisture, there was no significant absorption during these particular passes. Furthermore, the abnormal instrument response commonly observed when absorption occurs was not observed during these passes. Moreover, based on experience with the QCM under laboratory conditions, it appears that the smooth responses observed during passes 1, 6, and 7 indicate no problems were caused by moisture. Since the data from the other passes are not useful they are not presented.

Particles were also collected on the surface of filters mounted in an NASA aerosol concentrator described in reference 13. Ten filters were in a carrousel arrangement so that one filter could be exposed during each pass through the cloud up to 10 passes. The total mass concentrations and the mass concentrations of Al_2O_3 per pass were obtained using the procedure described later under "Surface Effluent Measurements." These results are presented in table XII. The filter wheel did not advance because of a mechanical problem between passes 3 and 4; therefore, the same filter was exposed for these two passes. However, since the time in the cloud was approximately the same for both passes, the total mass collected was divided by 2 to get the mass collected for each pass.

The collection efficiency in the concentrator is 50 percent for particles 1.0 μm in diameter and decreased with decreasing particle diameter, as noted in reference 13, so that particles smaller than 10 μm are not efficiently sampled. In-cloud size distribution measurements of reference 17 show that the larger percentage of the particles is smaller than 1 μm in diameter. Only a small percentage of these small particles is collected on the filters in the concentrator. On the other hand the particles larger than 1 μm in diameter are preferentially sampled so that a disproportionate number of large particles are collected on the filters. This tends to give an apparent higher mass concentration. Therefore, the mass concentration measured with this instrument is not representative of the true in-cloud concentrations.

Surface Effluent Measurements

Chemiluminescent detectors were deployed at all primary sites except P-9 (see table II) and measurable quantities of HCl effluents were recorded at sites P-2, P-3, and P-4. These chemiluminescent measurements are presented in figure 11. Also, pH paper was deployed at all sites with qualitative detection at sites P-6 and P-9. Likewise, there were filters at every site except P-9 to obtain particle data which are presented in table XIII.

Hydrogen chloride.- The chemiluminescent HCl measurements (with a detection limit of 0.005 ppm) and pH detection relative to the optically measured cloud track are presented in figure 12. The HCl highest peak concentration of 0.50 ppm was measured at the primary site closest to the launch pad, site P-4,

with the remaining HCl peak measurements decreasing with distance from the launch pad at sites P-2 and P-3, respectively. Some pH spotting was also noted at site P-9, which did not have a chemiluminescent detector, and at site P-6. Relative to the rate at which the optically tracked cloud moved, these HCl peak concentrations were measured prior to the time the ground cloud arrived in the vicinity of the instrument sites. (See fig. 12.) Since the part of the ground cloud which the aircraft sampled turned southerly shortly after launch (see fig. 9), it would not be expected to influence these surface measurements except possibly the pH spotting at site P-9.

Particles.- The surface filter particle measurements listed in table XIII consist of total mass concentration of particles, the mass concentration of Al_2O_3, and the percentage of Al_2O_3 measured at each instrument site. The sampling time for each filter is also given in the table. The standard stop times depended on the predicted cloud arrival time for each instrument site. The total mass concentration C is given by

$$C = \frac{W_C}{Qt} \tag{1}$$

with

$$W_C = (W_S - W_H) - \chi_A Qt \tag{2}$$

where

W_C corrected mass gain, μg

W_S uncorrected sample mass gain, μg

W_H handling effects correction factor, μg

χ_A normal ambient mass concentration, $\mu g/m^3$

Q sample flow rate, m^3/min

t sample time, min

The uncorrected sample mass gain W_S for each filter was obtained from prelaunch and postlaunch weighings in a Class 100 clean room. The handling effect W_H was found to be 55 μg from the average weight gained on 17 control filters that were not exposed during the sampling period. The normal ambient mass concentration measured on the day before launch was 32 $\mu g/m^3$. The pumps were adjusted such that the flow rate Q through each filter was 0.027 m^3/min.

The quantity of aluminum in each sample was determined by neutron activation analysis (NAA). According to the manufacturer's data each filter contains approximately 1 μg of aluminum; therefore, the weight of aluminum in the sample was obtained by subtracting 1 μg from the weight of aluminum given by NAA. It was assumed that all of the aluminum collected in the sample was in the form of Al_2O_3. The weight gain in Al_2O_3 is given by

$$W_{Al_2O_3} = 1.88W_{Al} \quad (3)$$

where $W_{Al_2O_3}$ is the weight of Al_2O_3 and W_{Al} is the weight of aluminum.

The mass concentration of Al_2O_3 is given by

$$C_{Al_2O_3} = \frac{W_{Al_2O_3}}{Qt} \quad (4)$$

Because of malfunctions, no particle-size distribution data were obtained with either of the two Climet or the Royco light scattering photometers. None of the quartz-crystal mass monitors indicated concentrations above the background levels throughout the sampling period. Filters from the Andersen cascade impactors did not show measurable weight increases nor did the high-volume filters because of the short sampling times. Therefore, the only quantitative data on the surface particulates were obtained with the filters.

Comparison of Model Predictions and Surface Measurements

For comparative purposes, postlaunch model predictions of HCl and Al_2O_3 levels from table XI and corresponding surface measurements from tables XIII and XIV are presented in table XV. Comparison of the predicted and measured values, on a point-to-point basis, reveals inconsistent results. From figure 9, it is noted that the optically tracked cloud path was approximately 10° off of the predicted path. Even considering the effect that a 10° uncertainty in cloud trajectory has upon the predicted effluent levels (see table XI) does not alter the inconsistency. The only agreement on a point-to-point basis, between the model predictions and measurements, appears to be in the location of the highest HCl concentration downwind from the launch pad. The highest predicted HCl concentration of 0.56 ppm was at P-9 located 5 km downwind of the pad. Although there was no HCl concentration instrument at P-9, the highest measured value of 0.50 ppm was obtained nearby at P-4 (see fig. 12) which was 4 km downwind of the pad. However, this agreement is not maintained when considering the other comparative values in table XV.

Reviewing all of the comparative values in table XV it is noted that in most cases, particularly for Al_2O_3, predictions are higher than the measured values. The results of another launch reported in reference 6 also noted that the model generally predicts high effluent values at the surface. However, since cloud separation was not taken into account in the predictions, this fact could influence results of comparing measurements to predicted values.

CONCLUDING REMARKS

A combination of surface and airborne effluent measuring instrumentation was deployed to determine the behavior of and effluent dispersion from the

ground cloud of a Titan III-E launched December 10, 1974, from the Air Force Eastern Test Range in Florida. These measurements are compared with diffusion model predictions to assess the applicability and accuracy of the model to determine the environmental impact of future launches.

The ground cloud from this launch rose at a rate of 4 m/sec compared with a predicted average value of 5 m/sec. Upon passing through a combined temperature inversion and wind shear layer at a 0.6-km altitude the cloud separated into at least two clouds. One cloud continued to rise above the predicted 0.82-km stabilization altitude to about 1.4 km but drifted in the predicted southeasterly direction. Another cloud, sampled by a specially instrumented aircraft, stabilized at approximately 0.07 km below the predicted 0.82-km altitude but traveled in an unpredicted southerly direction.

Although the nighttime launch created difficulty for the sampling aircraft to maintain necessary visual contact with the ground cloud, 20 passes were made through the southerly moving cloud during the period 3 to 55 min after launch. The highest effluent levels measured were 45 ppm HCl and 371 $\mu g/m^3$ Al_2O_3 5 min after launch. During the last pass a HCl peak value of 25 ppm was measured. No diffusion-model predictions are available for comparison with these measured effluent values.

The highest HCl measurement obtained by the instrumented surface sites, which were located near the path of the southeasterly moving cloud, was 0.50 ppm 4 km from the launch pad. The remaining HCl concentrations measured decreased with distance from the pad. The highest Al_2O_3 mass concentration of 1274 $\mu g/m^3$ was measured on the launch pad. The remaining Al_2O_3 measurements varied between 168 to 1.2 $\mu g/m^3$ but did not decrease consistently with distance from the pad. A point-to-point comparison of surface measurements with diffusion-model predicted effluent levels was also inconsistent. The only direct comparison appears to be in the location of the highest HCl concentration downwind of the pad, a measured value of 0.50 ppm 4 km from the pad compared with a predicted value of 0.56 ppm 5 km from the pad. Overall comparison of the measured and predicted effluent levels, particularly Al_2O_3, shows that the model tends to overpredict effluent levels.

Langley Research Center
National Aeronautics and Space Administration
Hampton, VA 23665
August 31, 1978

REFERENCES

1. Stephens, J. Briscoe; and Hamilton, P. A.: Diffusion Algorithms and Data Reduction Routine for Onsite Launch Predictions for the Transport of Titan III C Exhaust Effluents. NASA TN D-7862, 1974.

2. Gregory, Gerald L.; and Storey, Richard W., Jr.: Effluent Sampling of Titan III C Vehicle Exhaust. NASA TM X-3228, 1975.

3. Stewart, Roger B.; Sentell, Ronald J.; and Gregory, Gerald L.: Experimental Measurements of the Ground Cloud Effluents and Cloud Growth During the February 11, 1974 Titan-Centaur Launch at Kennedy Space Center. NASA TM X-72820, 1976.

4. Bendura, Richard J.; and Crumbly, Kenneth H.: Ground Cloud Effluent Measurements During the May 30, 1974, Titan III Launch at the Air Force Eastern Test Range. NASA TM X-3539, 1977.

5. Hulten, William C.; Storey, Richard W.; Gregory, Gerald L.; Woods, David C.; and Harris, Franklin S., Jr.: Effluent Sampling of Scout "D" and Delta Launch Vehicle Exhausts. NASA TM X-2987, 1974.

6. Gregory, Gerald L.; and Storey, Richard W., Jr.: Experimental Measurements of the Ground Cloud Effluents and Cloud Growth for the May 20, 1975, Titan IIIC Launch at Air Force Eastern Test Range, Florida. NASA TM-74044, 1977.

7. Environmental Statement for the Space Shuttle Program - Final Statement. NASA TM X-68541, 1972.

8. Stephens, J. Briscoe, ed.: Atmospheric Diffusion Predictions for the Exhaust Effluents From the Launch of a Titan IIIC, Dec. 13, 1973. NASA TM X-64925, 1974.

9. Gomberg, Richard I.; and Stewart, Roger B.: A Computer Simulation of the Afterburning Processes Occurring Within Solid Rocket Motor Plumes in the Troposphere. NASA TN D-8303, 1976.

10. AFETR Instrumentation Handbook. ETR-TR-71-5, U.S. Air Force, Sept. 1971. (Available from DDC as AD 735 263.)

11. Gregory, Gerald L.; Hudgins, Charles H.; and Emerson, Burt R., Jr.: Evaluation of a Chemiluminescent Hydrogen Chloride and a NDIR Carbon Monoxide Detector for Environmental Monitoring. 1974 JANNAF Propulsion Meeting, Volume I, Part II, CPIA Publ. 260 (Contract N00017-72-C-4401), Appl. Phys. Lab., Johns Hopkins Univ., Dec. 1974, pp. 681-704. (Available from DDC as AD B002 590.)

12. Reyes, Robert J.; Miller, Richard L.; and Beatty, David C.: Monitoring of HCl From Solid Propellant Launch Vehicles. 1974 JANNAF Propulsion Meeting, Volume I, Part II, CPIA Publ. 260 (Contract N00017-72-C-4401), Appl. Phys. Lab., Johns Hopkins Univ., Dec. 1974, pp. 705-722. (Available from DDC as AD B002 590.)

13. Wornom, Dewey E.; Woods, David C.; Thomas, Mitchel E.; and Tyson, Richard W.: Instrumentation of a Sampling Aircraft for Measurement of Launch Vehicle Effluents. NASA TM X-3500, 1977.

14. Stephens, J. Briscoe; Adelfang, S. I.; and Goldford, A. I.: Compendium of Meteorological Data for the Helios A Launch in December 1974. NASA TM X-73337, 1976.

15. Charlson, R. J.; Ahlquist, N. C.; Selvidge, H.; and MacCready, P. B., Jr.: Monitoring of Atmospheric Aerosol Parameters With the Integrating Nephelometer. J. Air Pollution Control Assoc., vol. 19, no. 12, Dec. 1969, pp. 937-942.

16. Woods, David C.: The Effects of Particle Size Distribution and Refractive Index on Aerosol Mass Concentration Measurements Made With an Integrating Nephelometer. Blacks in Technology - Beyond the Bicentennial, CP 101, Natl. Tech. Assoc., Aug. 1977.

17. Woods, D. C.: Rocket Effluent Size Distributions Made With a Cascade Quartz Crystal Microbalance. Proceedings of the 4th Joint Conference on Sensing of Environmental Pollutants (New Orleans, LA), Nov. 6-11, 1977, pp. 716-718.

TABLE I.- TITAN SRM EXHAUST COMPOSITION

[Percent by mass of flow]

Product	At nozzle exit plane (a)	At 1 km from exit plane (b)
Aluminum oxide (Al_2O_3)	30.4	30.4
Carbon monoxide (CO)	27.9	(c)
Hydrogen chloride (HCl)	21.0	20.4
Nitrogen (N_2)	8.4	(d)
Water vapor (H_2O)	6.7	31.9
Carbon dioxide (CO_2)	2.9	48.0
Chlorine (Cl_2)	(c)	2.3
Oxygen (O_2)	(c)	(d)
Nitrogen oxide (NO)	(c)	1.2
Others	2.7	.6
	100.0	[e]134.8

[a]Data from reference 8.
[b]Data from reference 9.
[c]Less than 0.1.
[d]Assumed to be part of air.
[e]Total greater than 100 percent because of chemical addition of air in afterburning.

TABLE II.- SURFACE SAMPLING INSTRUMENTATION

Instrument	Species	Sites											
		Primary									Secondary	Fallback	Tower
		P-1	P-2	P-3	P-4	P-5	P-6	P-7	P-8	P-9	S-1 to S-30	1 to 3	
Chemiluminescent detector	HCl	X	X	X	X	X	X	X	X				
Bubbler	HCl	X	X	X	X	X	X	X	X	X	X	X	X
Microcoulometer	HCl	X							X				
pH paper	HCl	X	X	X	X	X	X	X	X	X	X	X	X
Mass monitor	Particles	X	X	X	X	X	X	X	X				
Concentrator filter	Particles	X	X	X	X	X	X	X	X		X	X	X
Andersen cascade impactor	Particles	X	X	X	X	X	X	X	X				
Climet photometer	Particles	X	X										
Light photometer	Particles			X									
High volume cascade impactor	Particles											X	X
Nondispersive infrared detector	CO	X			X	X			X	X			
Infrared gas analyzer	CO_2								X	X			

TABLE III.- CAPABILITIES OF SURFACE SAMPLING INSTRUMENTS

(a) Gas instruments

Instrument/Species	Range	Detection limit	Response to 90-percent reading	Required analysis
Chemiluminescent detector/HCl (ref. 9)	0.005 to 50 ppm	0.05 ppm	1 to 5 sec	None
Microcoulometer/HCl (ref. 12)	0.1 to 20 ppm	0.1 ppm	1 to 5 sec	None
Bubbler/HCl (ref. 5)	>80 ppm-sec	80 ppm-sec	NA	Coulometric
pH paper/HCl (ref. 5)	Qualitative	1 ppm	NA	None
[a]Infrared gas analyzer/CO_2	1 to 50 ppm above ambient	1 ppm above ambient	2.5 sec	None
Nondispersive infrared detector/CO (ref. 11)	0.5 to 200 ppm	0.5 ppm	28 sec	None

(b) Particle instruments

Instrument (b)	Range (μm diameter)	Detection limit	Response to 90-percent reading	Required analysis
Royco photometer	0.5 to 6.5	1 particle	1 msec	Computer processing
Climet photometer	0.3 to 10.0	1 particle	1 msec	Computer processing
Mass monitor	0.1 to 20.0	10 $\mu g/m^3$	5 sec	None
Concentrator filter	>0.1	10 μg	NA	Gravimetric and NAA
High volume cascade impactor	>0.01	200 μg	NA	Gravimetric and NAA
Andersen cascade impactor	0.43 to 11.0	50 μg	NA	Gravimetric and NAA

[a]Instrument specifications based on manufacturer's data.
[b]Instrument specifications from manufacturer's data or field experience (ref. 5).

TABLE IV.- CAPABILITIES OF AIRBORNE SAMPLING INSTRUMENTS

Instrument/Species	Range	Detection limit	Response, 90 percent of full scale reading	Required analysis
Chemiluminescent detector/HCl	0 to 200 ppm	0.1 ppm	1 sec	None
Mass monitor/Particles	0 to 2000 $\mu g/m^3$	3 $\mu g/m^3$	2 sec	None
Integrating nephelometer/ Particles	0 to 3800 $\mu g/m^3$	9 $\mu g/m^3$	0.2 sec	None
Concentrator (filter)/ Particles	NA	NA	NA	NAA

TABLE V.- PRELAUNCH CLOUD PREDICTIONS

Time	Cloud-stabilization altitude, km	Cloud path from LC-41, deg	HCl peak concentrations, ppm	Location of peak from LC-41, km
T-24 hr	1.828	158	1.2	7.5
T-14 hr	2.100	147	1.3	6.6
T-9 hr	-----	150	---	5.6
T-6 hr	-----	185	---	6.2
T-3 hr	1.828	150	1.3	6.0

TABLE VI.- DEPLOYMENT AND OPERATIONAL TIMES FOR SURFACE INSTRUMENTS

Site	Instrument	Site assignment	Model prediction	Instrument in place	Instrument ready to sample	Background sample	Sampling period	
							Start	Stop
Tower	Bubbler	T-2 days	T-2 days	T-2 days	T-6 hr	NA	T-1 min	T+5 min
	pH paper					NA	T-6 hr	T+1 hr
	Concentrator					T+1 day	T-1 min	T+5 min
	Andersen cascade impactor No. 1					T+1 day	T-1 min	T+30 sec
	Andersen cascade impactor No. 2					T+1 day	T+30 sec	T+5 min
	High volume cascade impactor					T+1 day	T-1 min	T+5 min
Fallback	Bubbler	T-1 day	T-1 day	T-1 day	T-4$\frac{1}{2}$ hr	NA	T-1 min	T+5 min
	pH					NA		
	Concentrator					T+1 day		
	High volume cascade impactor					T+1 day		
Secondary	Bubbler	T-6 hr	T-8 hr	T-2$\frac{1}{2}$ hr	T-2 hr	NA	Inoperative	
	pH					NA	T-6 hr	T+1 hr
	Concentrator					T+1 day	Inoperative	
Primary	Chemiluminescent detector	Seacraft: T-9 hr	Seacraft: T-14 hr	Seacraft: T-2$\frac{1}{2}$ hr	T-1 hr	T-30 min, T+2 hr	[a]T-30 min	As directed
	Bubbler No. 1	Land: T-4$\frac{1}{2}$ hr	Land: T-6 hr	Land: T-4 hr		NA	T-60 min	T-3 min
	Bubbler No. 2					NA	As directed	As directed
	Microcoulometer					T-30 min, T+2 hr	As directed	As directed
	pH					NA	T-3 min	As directed
	Mass monitor					T-15 min	T-30 min	As directed
	Concentrator					NA	As directed	As directed
	Andersen cascade impactor					NA	As directed	As directed
	Climet photometer					T-15 min	Inoperative	
	Royco photometer					T-15 min	Inoperative	
	Nondispersive infrared detector					T-30 min, T+2 hr	T-30 min	As directed
	Infrared gas analyzer					T-30 min, T+2 hr	T-30 min	As directed

[a]P-6 chemiluminescent instrument inoperative.

TABLE VII.- SURFACE-INSTRUMENT LOCATIONS RELATIVE TO LAUNCH COMPLEX 41

Site	Azimuth, deg	Distance from LC-41, km
Tower	90	0.1
Fallback 1	136	1.3
Fallback 2	160	2.1
Fallback 3	164	2.1
P-1	147	7
P-2	130	7
P-3	147	11.5
P-4	147	4
P-5	147	15
P-6	165	9
P-7	163	12.5
P-8	163	14
P-9	160	5
[a]S-1	167.6	6.3
S-2	159.8	5.5
S-3	171.9	8.7
S-4	163.6	8.9
S-5	174.7	9.3
S-6	162.9	10.1
S-7	168.8	10.8
S-8	162.4	11.3
S-9	161.7	12.5
S-10	162.6	14.1
S-11	165.8	14.7
S-12	159.5	15.3
S-13	163	15.7
S-14	163.4	10.9
S-15	175.1	13.5
S-16	177.5	11.9
S-17	174.5	12.5
S-18	171.9	13.1
S-19	170	13.5
S-20	168.4	14.0
S-21	183.2	15.2
S-22	179.5	15.2
S-23	168.4	15.1
S-24	174.4	15.1
S-25	171.8	15.8
S-26	173.9	16.1
S-27	177.7	16.5
S-28	181.1	16.5
S-29	184.2	16.5
S-30	176.6	15.1

[a]No bubbler or concentrator data obtained at secondary sites due to malfunction of remote activation system.

TABLE VIII.- AIRCRAFT SAMPLING PARAMETERS

Pass number	Sampling altitude, km (a)	Aircraft heading, deg (b)	Cloud-centroid location relative to launch pad (c)		Time of pass, T+min:sec (d)	
			Distance, km	Azimuth, deg	In	Out
1	1.080	61 to 71	1.77	164	3:18	3:32
2	.743	144 to 150	3.24	172	5:05	5:35
3	.674	15 to 50	-----	---	6:54	7:20
4	.759	128 to 152	-----	---	8:01	8:37
5	.740	19 to 46	-----	---	9:40	10:10
6	.742	120 to 130	-----	---	11:38	11:54
7	.678	299 to 348	-----	---	12:33	13:06
8	.485	238 to 260	-----	---	16:32	17:01
9	.534	20 to 81	-----	---	17:45	18:15
10	.576	286 to 295	18.51	182	28:21	29:32
11	.556	355 to 357	20.95	185	31:54	32:52
12	.568	60 to 140	23.39	182	34:30	35:34
13	.610	359 to 1	21.04	177	35:53	36:45
14	.553	161 to 210	23.17	185	37:32	38:52
15	.563	312 to 318	24.47	182	40:12	41:08
16	.551	156 to 226	25.95	184	43:06	44:30
17	.540	356 to 1	27.16	183	45:36	46:42
18	.511	186 to 294	30.03	184	48:30	49:46
19	.531	149 to 342	32.72	184	52:48	53:33
20	.548	344 to 354	32.25	180	55:04	55:46

[a]Referenced to mean sea level.

[b]Variation of aircraft heading while in cloud.

[c]From radar tracking data using midpoint times of nephelometer reading during pass. Radar acquisition during passes 3 to 9 was lost because the aircraft was in the vicinity of the radar location.

[d]Based on nephelometer response.

TABLE IX.- POSTLAUNCH PREDICTED CLOUD RISE AND STABILIZATION

Time after launch, T+min:sec	Cloud-centroid altitude, km
0:8.9	0.1929
0:11.8	.2265
0:19.9	.3048
0:58.9	.5568
1:11.0	.6096
1:12.8	.6166
1:25.8	.6611
[a]2:45.9	[a].8194

[a]Stabilization conditions: 1.609 km and azimuth of 170° from LC-41.

TABLE X.- POSTLAUNCH PREDICTED CLOUD TRACK AND GROWTH

Time after launch, T+min:sec	Cloud-centroid location relative to LC-41		Cloud dimensions	
	Azimuth, deg	Distance, km	Crosswind, km	Alongwind, km
3:15.9	167	0.0341	1.049	1.049
7:45.9	160	2.892	1.202	3.295
12:45.9	160	5.444	1.576	4.786
17:45.9	160	7.995	2.052	6.556
22:45.9	160	10.547	2.575	8.432
27:45.9	160	13.098	3.121	10.356
32:45.9	160	15.650	3.681	12.305
37:45.9	160	18.202	4.248	14.270
42:45.9	160	20.753	4.820	16.244
47:45.9	160	23.305	5.395	18.225
52:45.9	160	25.857	5.973	20.211
57:45.9	160	28.408	6.552	22.199
62:45.9	160	30.960	7.134	24.191

TABLE XI.- POSTLAUNCH MODEL PREDICTION OF HCl AND Al_2O_3 CONCENTRATIONS AND DOSAGES AT PRIMARY SURFACE INSTRUMENT SITES[a]

Site	HCl		Al_2O_3	
	Maximum concentration, ppm	Dosage, ppm-sec	Maximum concentration, mg/m^3	Dosage, $mg\text{-}sec/m^3$
P-1	0.27 ± 0.02	33.5 ± 2.5	620 ± 40	77.3 ± 5.8
P-2	0.01 ± 0.04	0.7 ± 4.5	10 ± 80	1.7 ± 10.3
P-3	0.15 ± 0.01	27.0 ± 1.8	330 ± 20	62.2 ± 4.1
P-4	0.22 ± 0.02	19.9 ± 1.7	500 ± 40	45.0 ± 4.0
P-5	0.09 ± 0.00	21.1 ± 1.4	210 ± 10	48.6 ± 3.1
P-6	0.56 ± 0.17	57.3 ± 18.1	860 ± 230	132.1 ± 41.7
P-7	0.24 ± 0.07	48.4 ± 14.9	540 ± 160	111.4 ± 34.4
P-8	0.19 ± 0.06	43.4 ± 13.5	440 ± 130	100.1 ± 31.1
P-9	0.37 ± 0.10	57.5 ± 15.5	1280 ± 400	132.6 ± 35.7

[a]± indicates the variance in the values stated for a ±10° uncertainty in cloud trajectory.

TABLE XII.- FILTER PARTICLE DATA FROM SAMPLING AIRCRAFT

Pass	Total mass concentration, $\mu g/m^3$	Al_2O_3 mass concentration, $\mu g/m^3$	Al_2O_3, percent of total
Background	30	0.3	1.0
1	4312	218.7	5.0
2	1000	329.9	33.0
[a]3	536	371.3	69.3
[a]4	536	371.3	69.3
5	2612	297.8	11.4
6	2638	118.9	4.5
7	608	53.2	8.8

[a]Same filter used for passes 3 and 4. Resulting weight was equally divided between the two passes.

TABLE XIII.- FILTER PARTICLE SURFACE MEASUREMENTS

Site	Sampling, time, min	Total mass concentration, $\mu g/m^3$	Al_2O_3 mass concentration, $\mu g/m^3$	Al_2O_3, percent of total
P-1	30	185	18.4	10.0
P-2	---	----	------	----
P-3	19	248	4.5	1.8
P-4	26	207	37.2	18.0
P-5	26	130	9.3	7.2
P-6	32	568	168.0	29.6
P-7	25	160	17.0	10.6
P-8	25	----	1.2	----
P-9	29	14	2.9	20.7
S-23	16	26	5.2	20.0
Fallback 1	6	146	------	----
Fallback 2	6	129	------	----
Tower	6	1656	1273.7	76.9

TABLE XIV.- SUMMARY OF PRIMARY SURFACE GAS MEASUREMENTS

Site	Concentration HCl, ppm	Dosage HCl, ppm-sec	pH paper	Odor detected
P-1	<0.005	----	----------	---
P-2	.35	19.5	----------	Yes
P-3	.022	6.2	----------	Yes
P-4	.50	15.2	----------	Yes
P-5	<.005	----	----------	---
P-6	------	----	Heavy spotting	Yes
P-7	<.005	----	----------	---
P-8	<.005	----	----------	---
P-9	------	----	Spotting	Yes

TABLE XV.- COMPARISON OF MODEL PREDICTIONS AND SURFACE MEASUREMENTS

Site	HCl				Al_2O_3	
	Measured		Predicted		Measured concentration, $\mu g/m^3$	Predicted concentration, $\mu g/m^3$
	Concentration, ppm	Dosage, ppm-sec	Concentration, ppm	Dosage, ppm-sec		
P-1	0.005	----	0.27	33.5	18.4	620
P-2	.350	19.5	.01	.7	-----	10
P-3	.022	6.2	.15	27.0	4.5	330
P-4	.500	15.2	.22	19.9	37.2	500
P-5	.005	----	.09	21.1	9.3	210
P-6	-----	----	.37	57.5	168.0	860
P-7	.005	----	.24	48.4	17.0	540
P-8	.005	----	.19	43.4	1.2	440
P-9	-----	----	.56	57.3	2.9	1280

Figure 1.- Titan III-C vehicle at lift-off, T+7 sec.

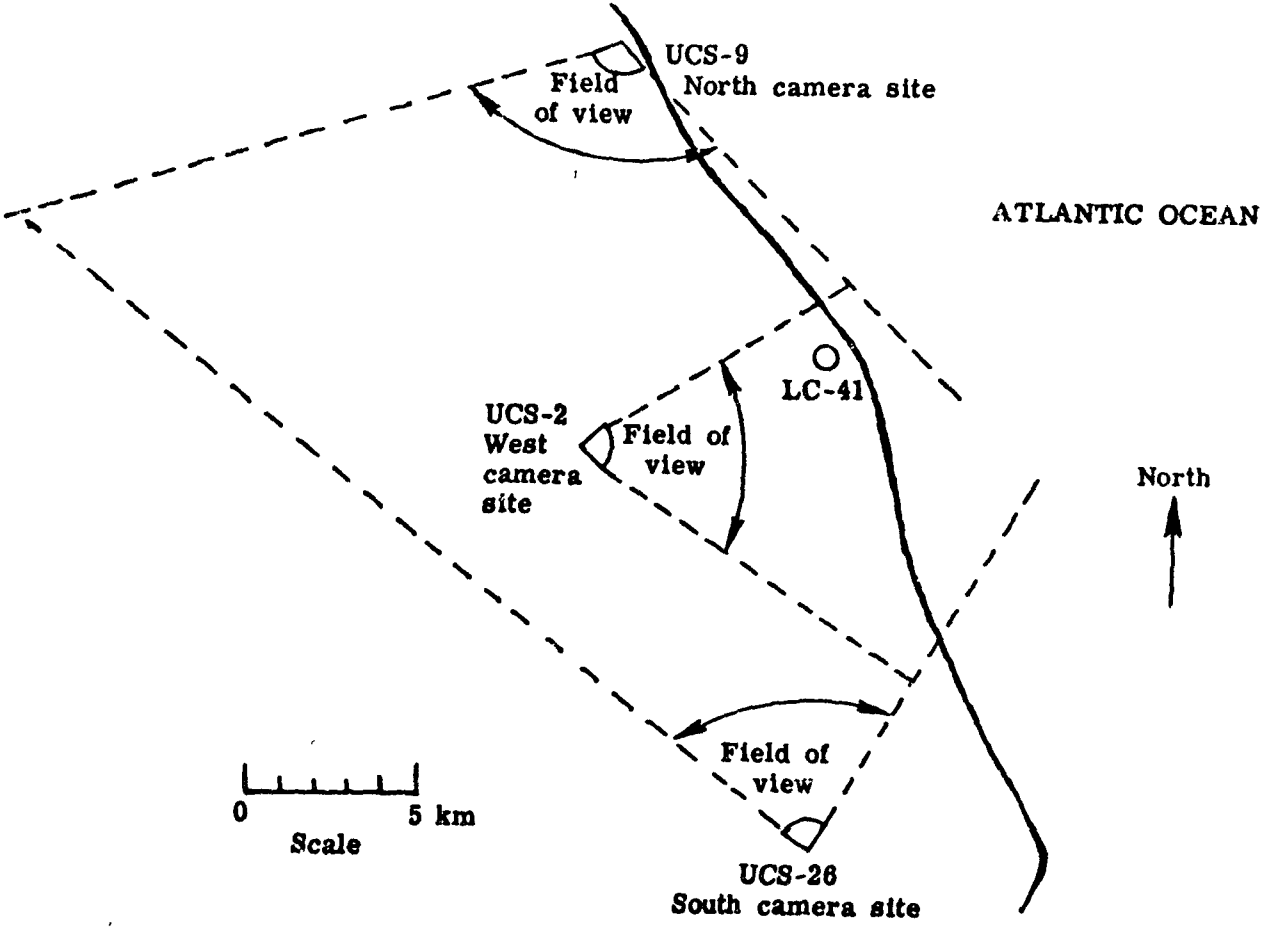

Figure 2.- Camera site plan.

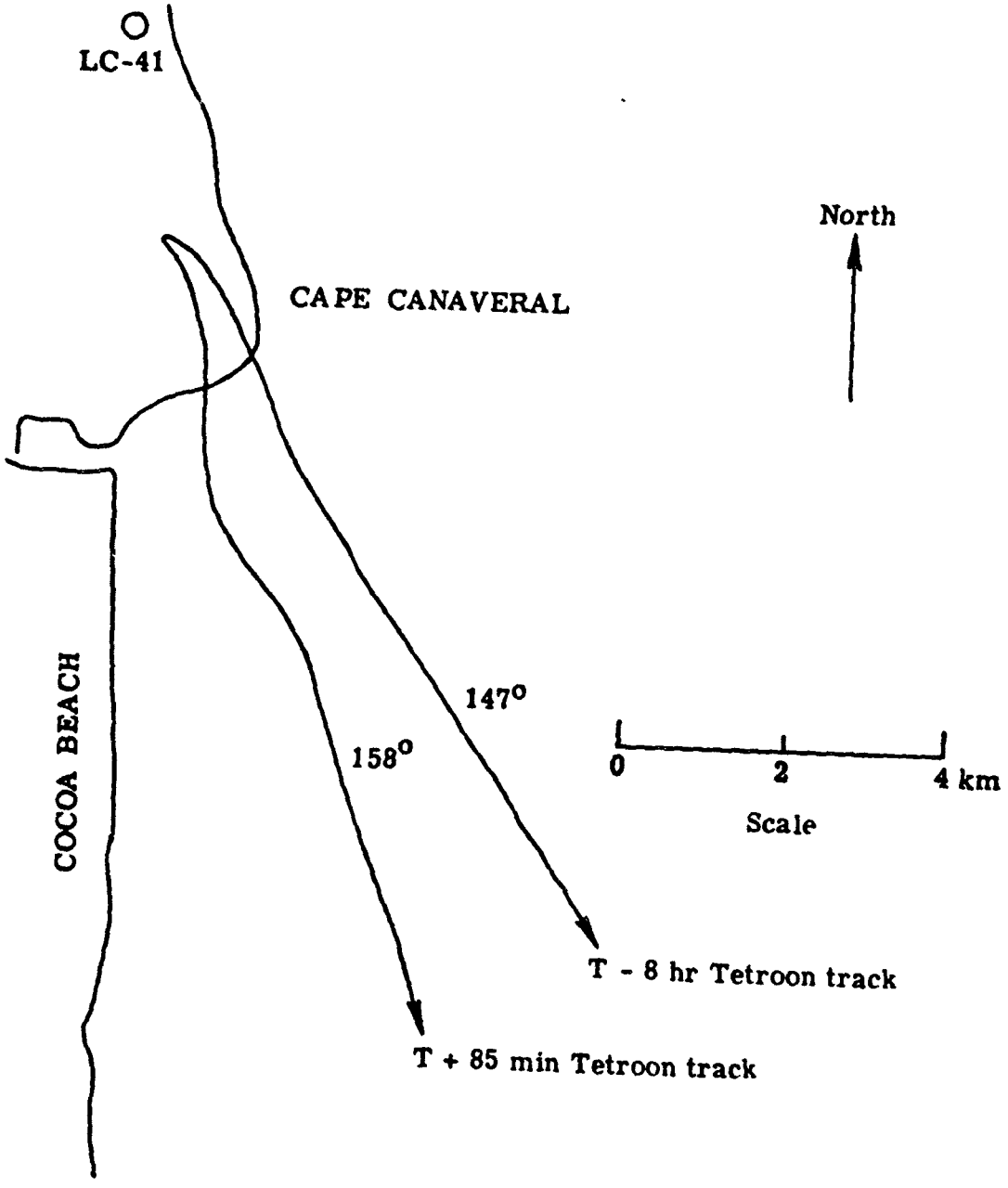

Figure 3.- Radar track of tetroon flights at a 0.82-km altitude.

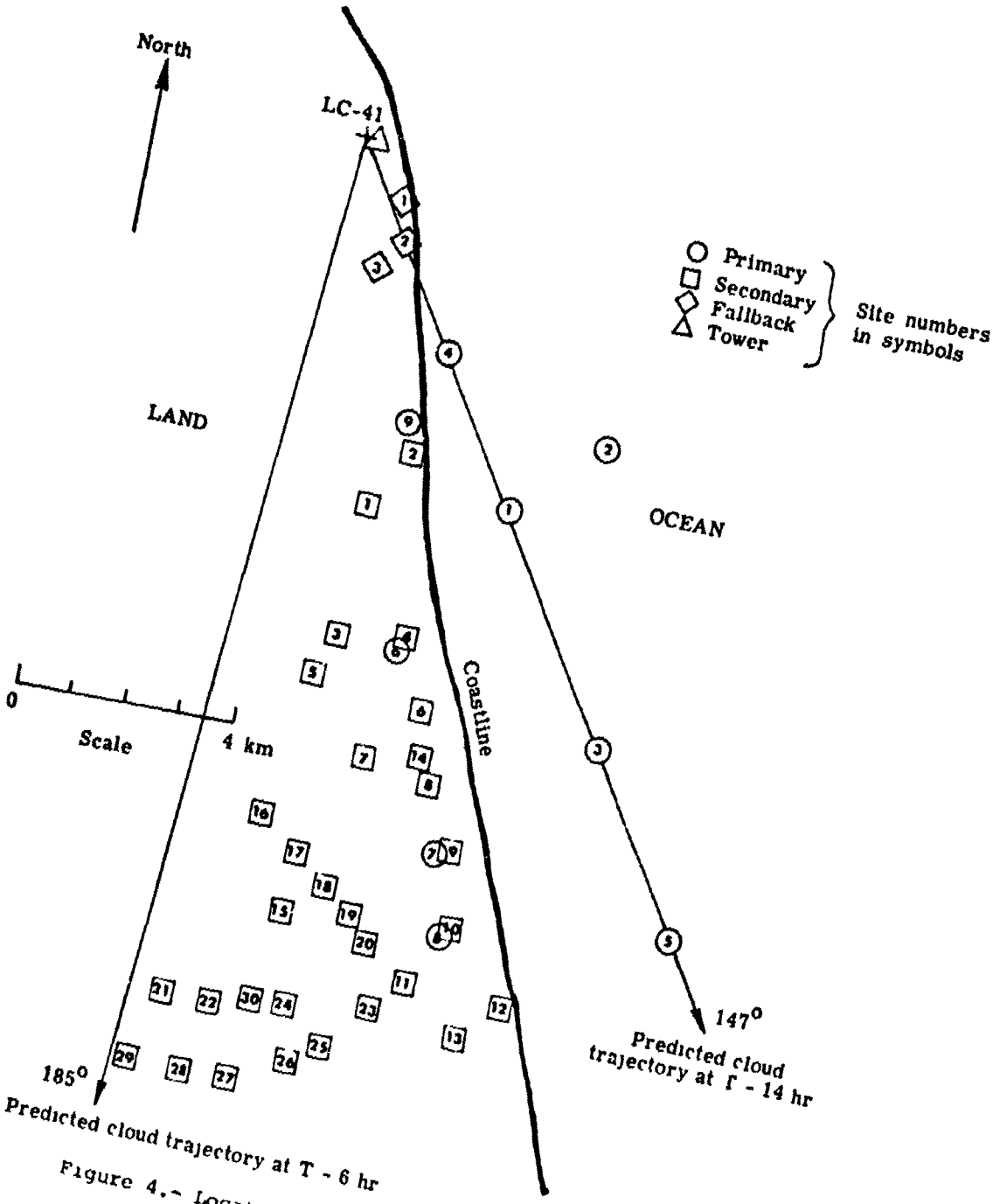

Figure 4.- Location of surface instrumentation.

L-77-196

Figure 5.- Aircraft cloud-sampling technique.

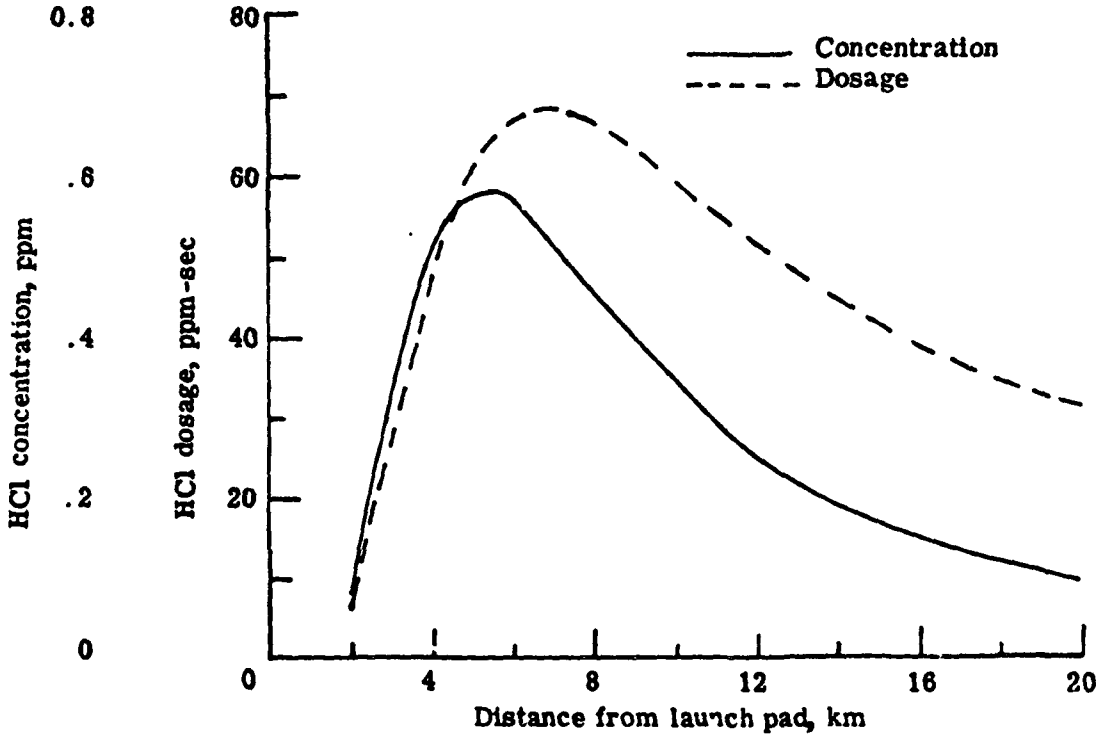

(a) Center-line values.

Figure 6.- Postlaunch model predictions.

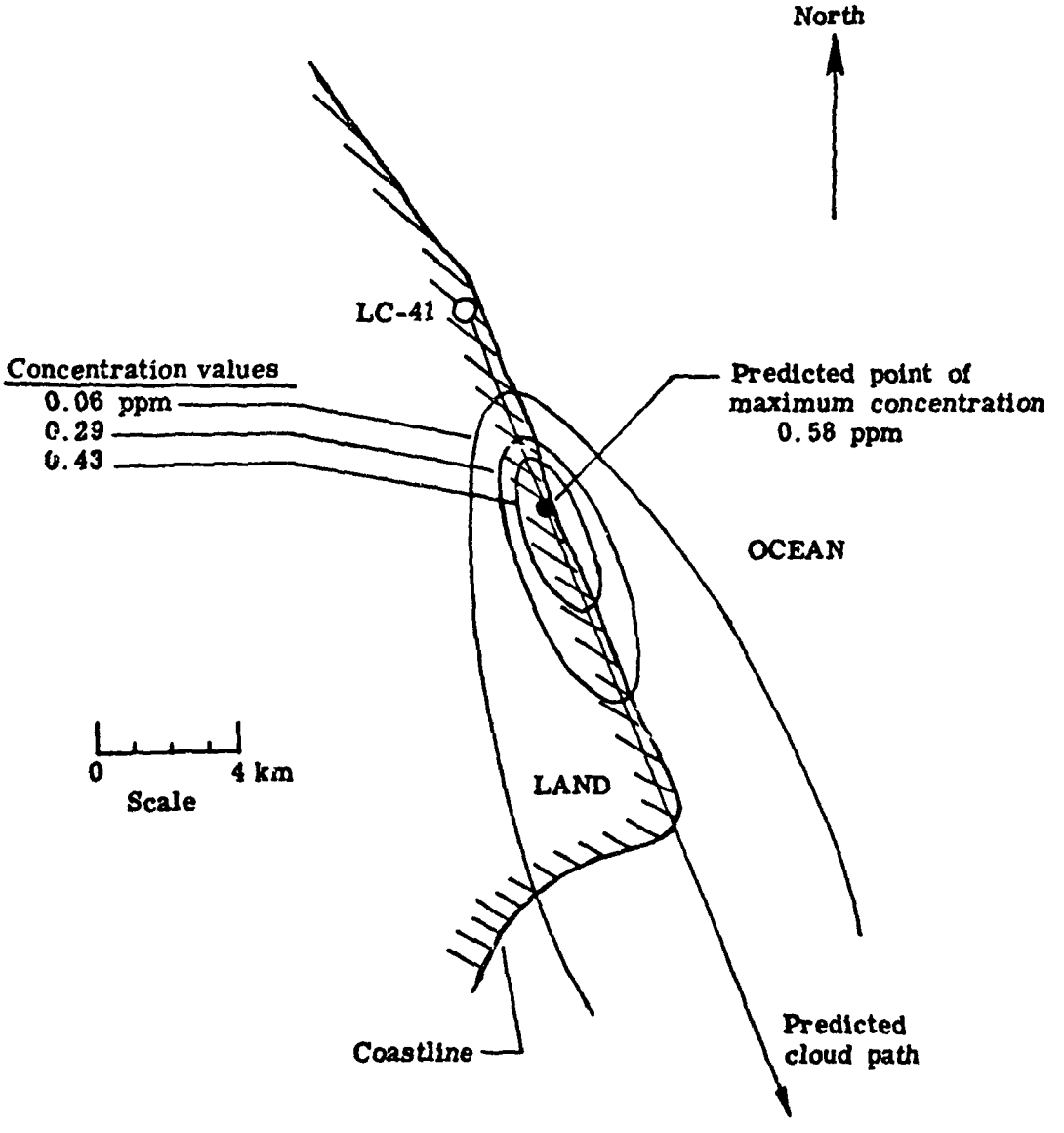

(b) Isopleths.

Figure 6.- Concluded.

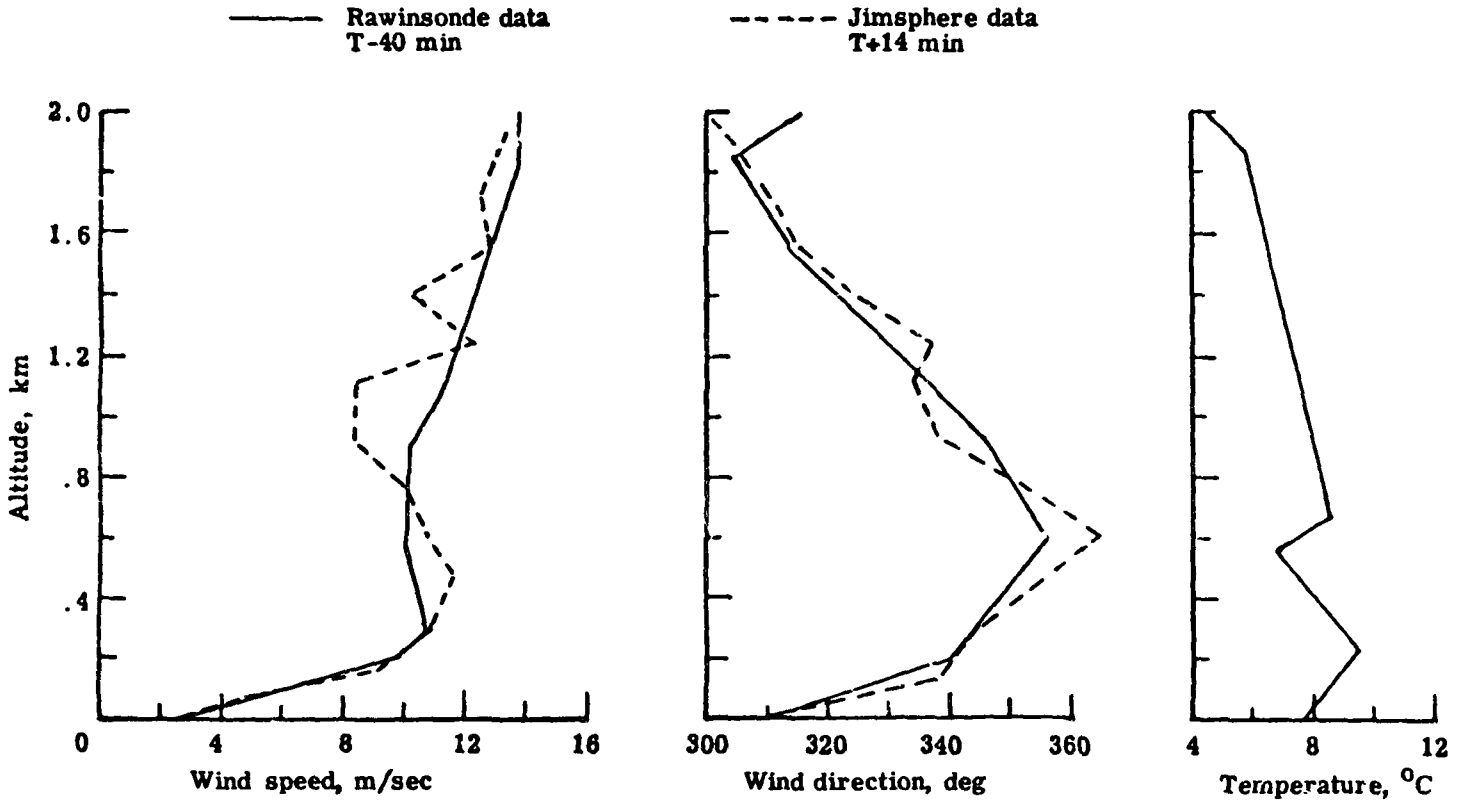

Figure 7.- Meteorological data for the December 10, 1974, Titan launch.

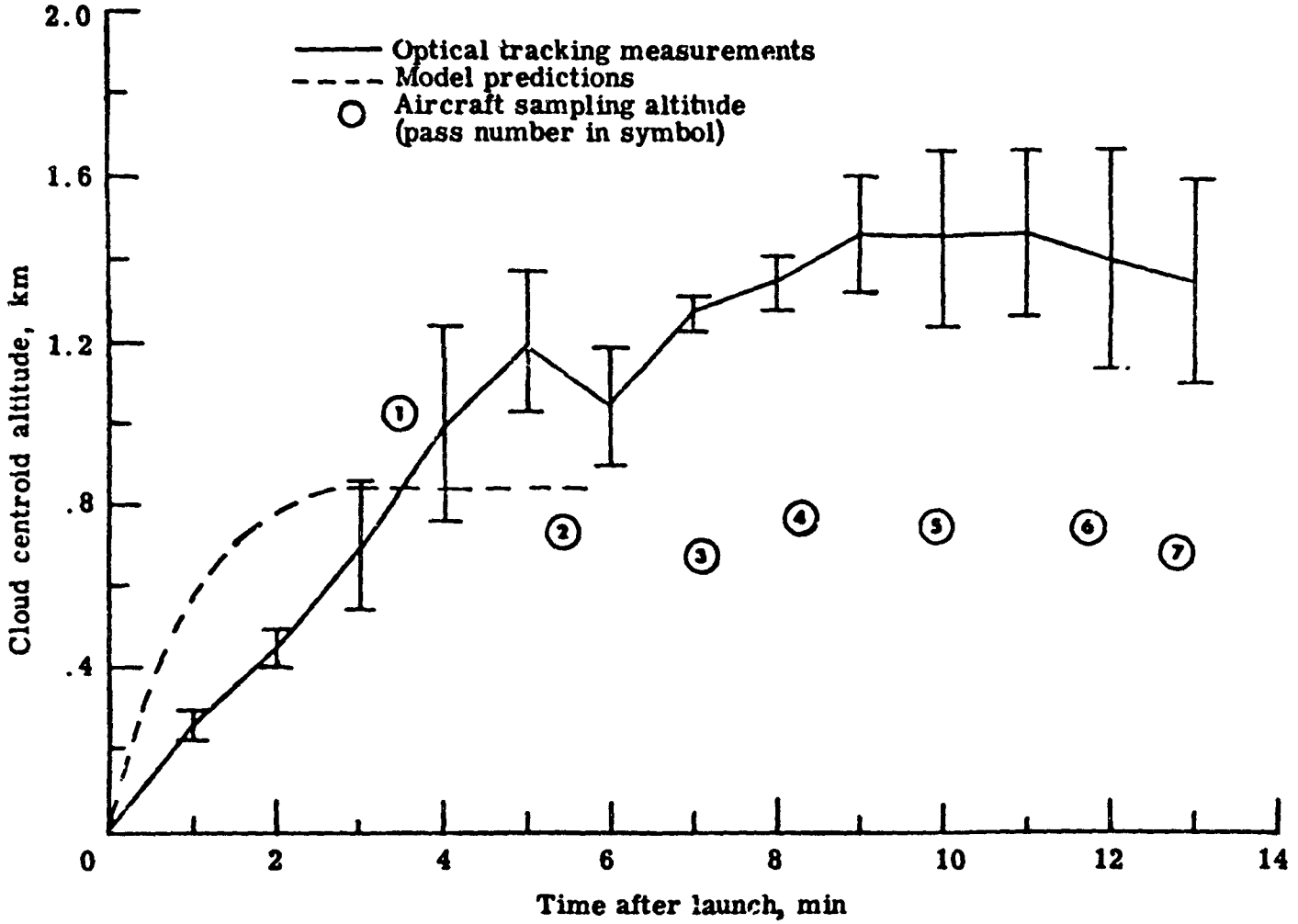

Figure 8.- Cloud rise and stabilization.

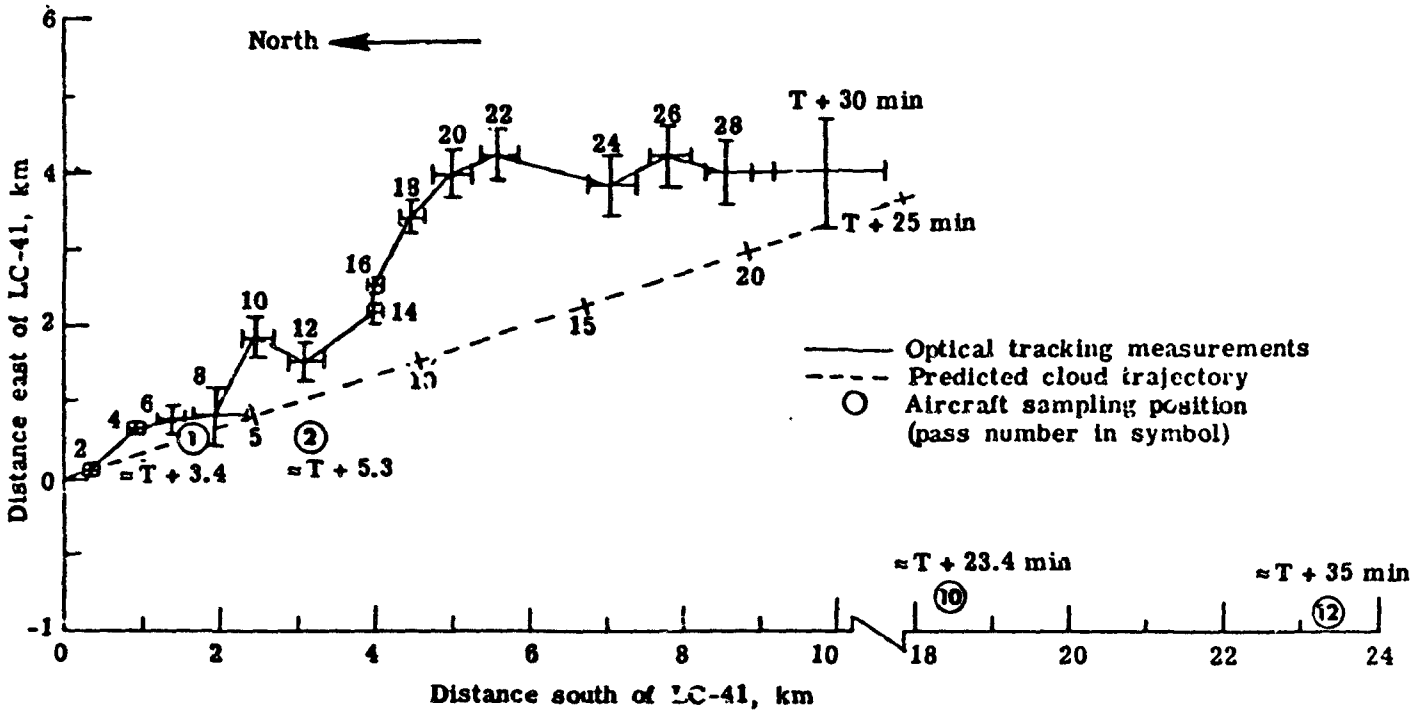

Figure 9.- Cloud ground trajectory.

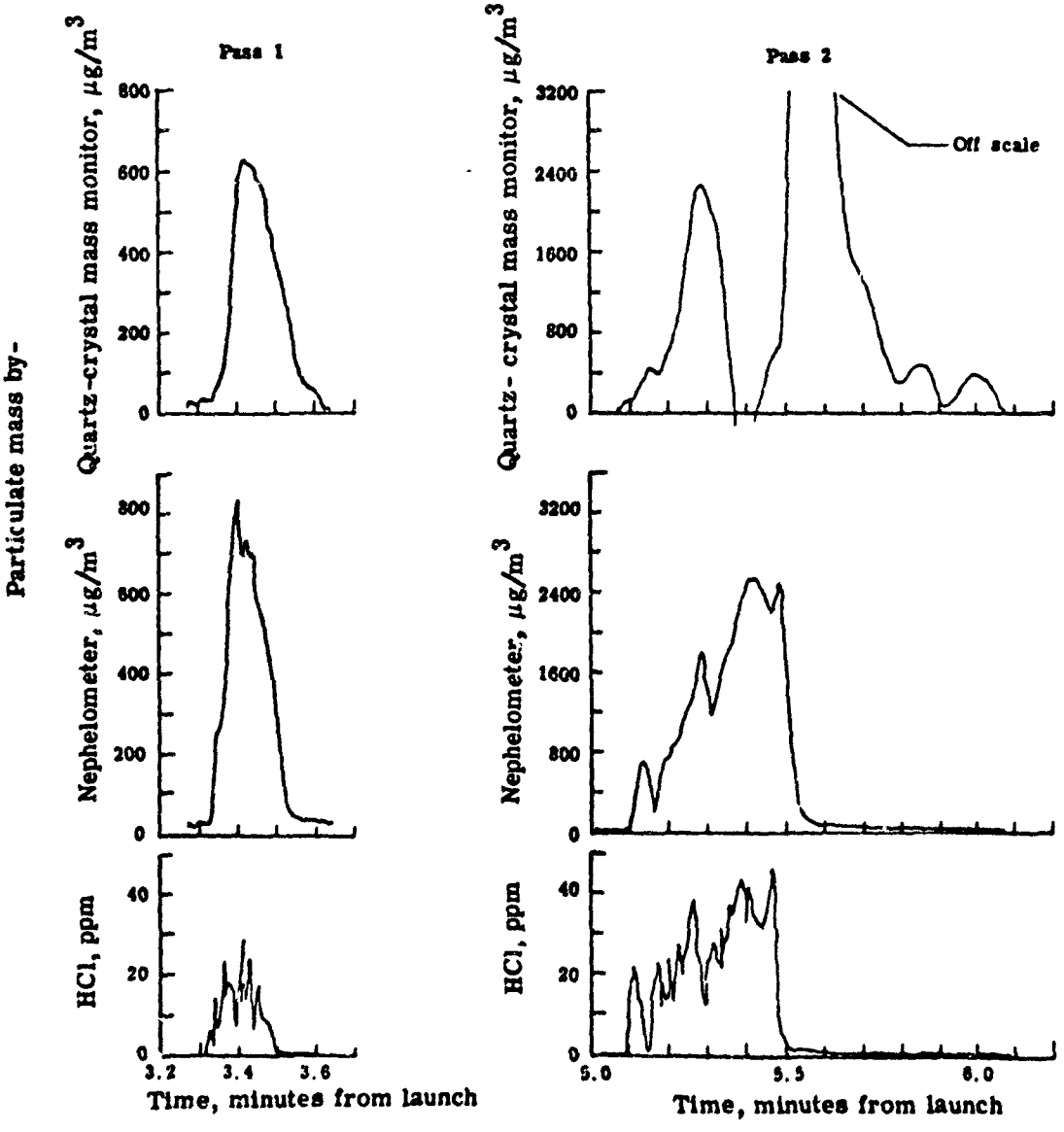

(a) Passes 1 and 2.

Figure 10.- In-cloud effluent measurement as obtained by the sampling aircraft.

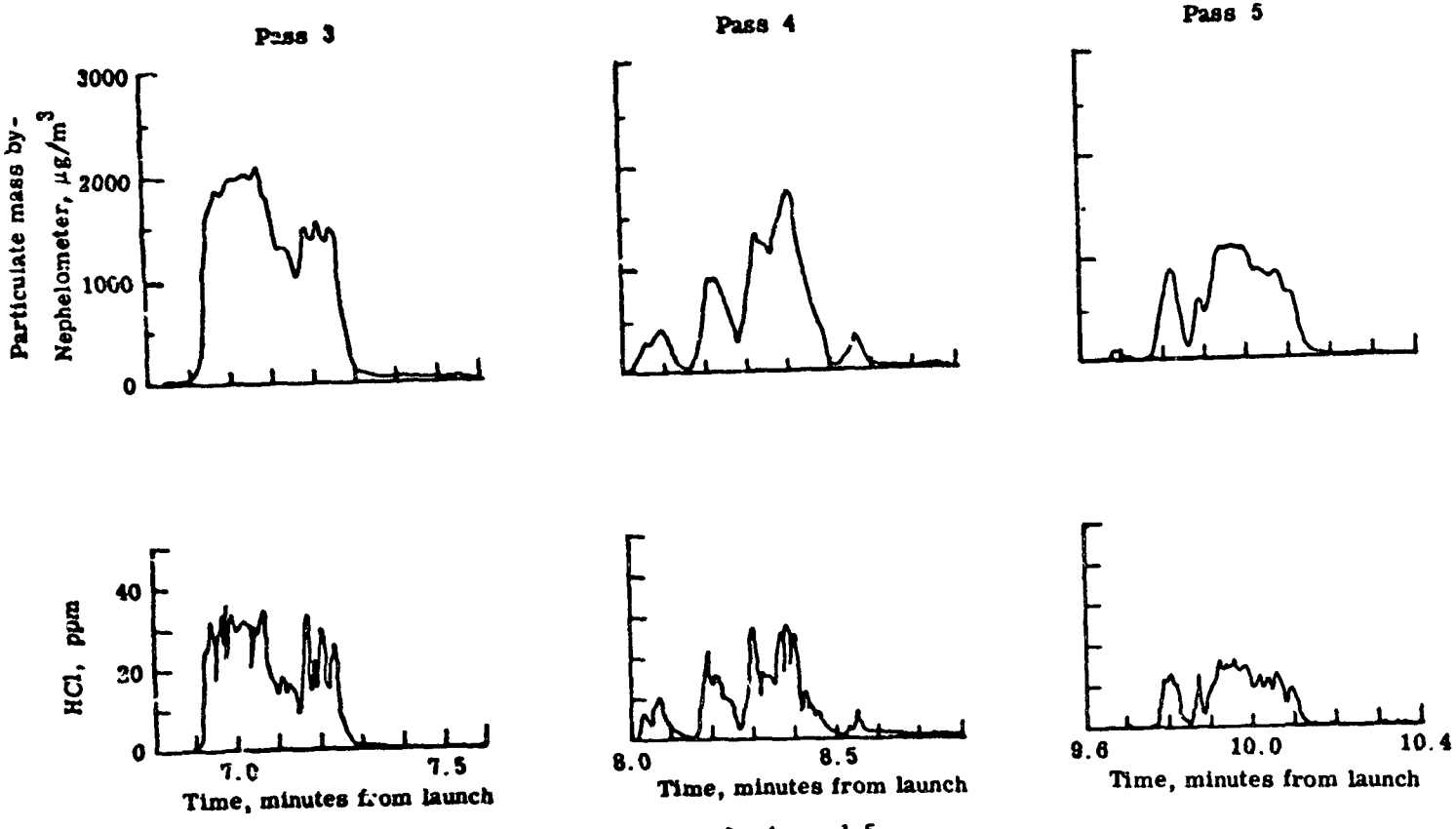

(b) Passes 3, 4, and 5.

Figure 10.- Continued.

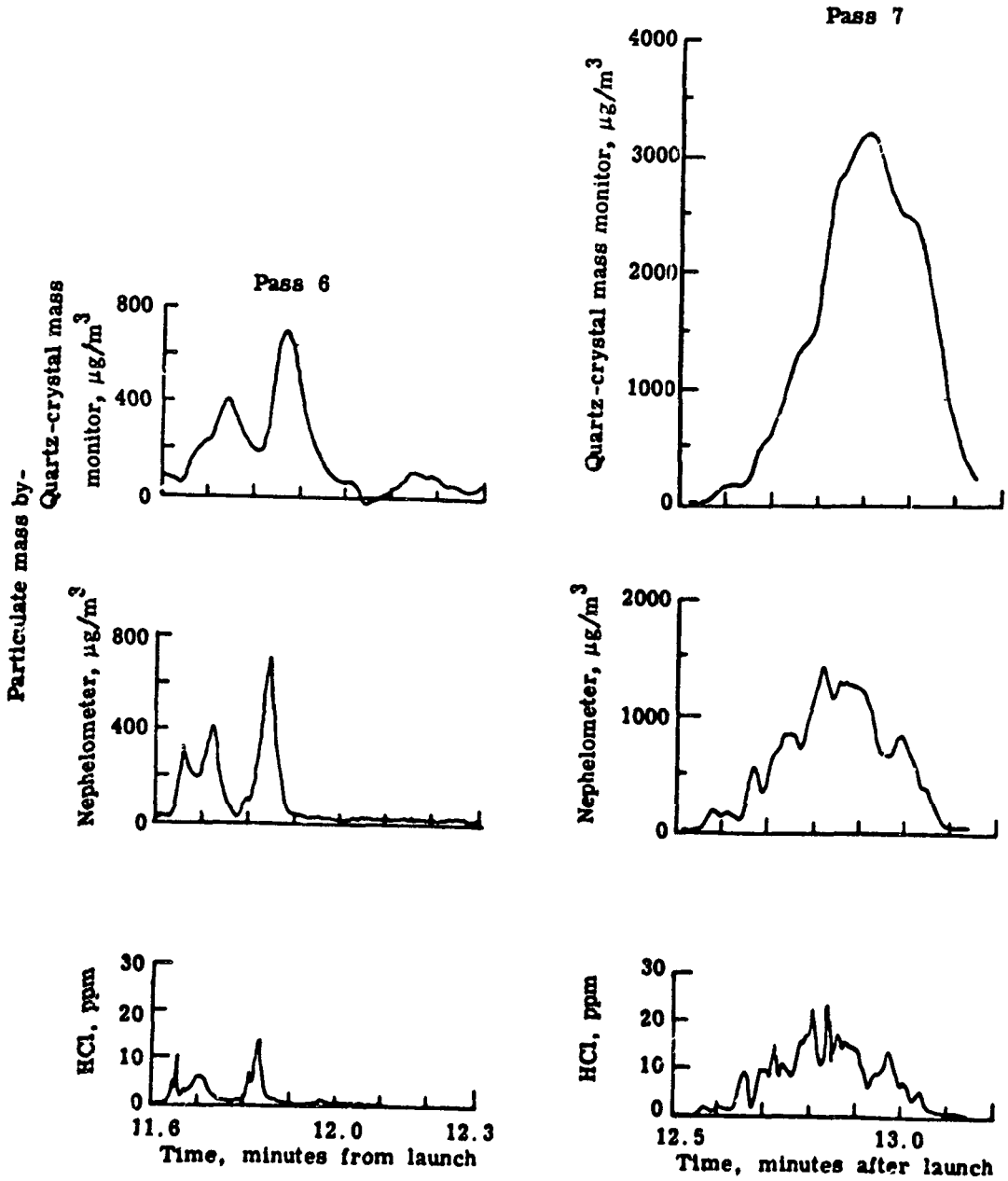

(c) Passes 6 and 7.

Figure 10.- Continued.

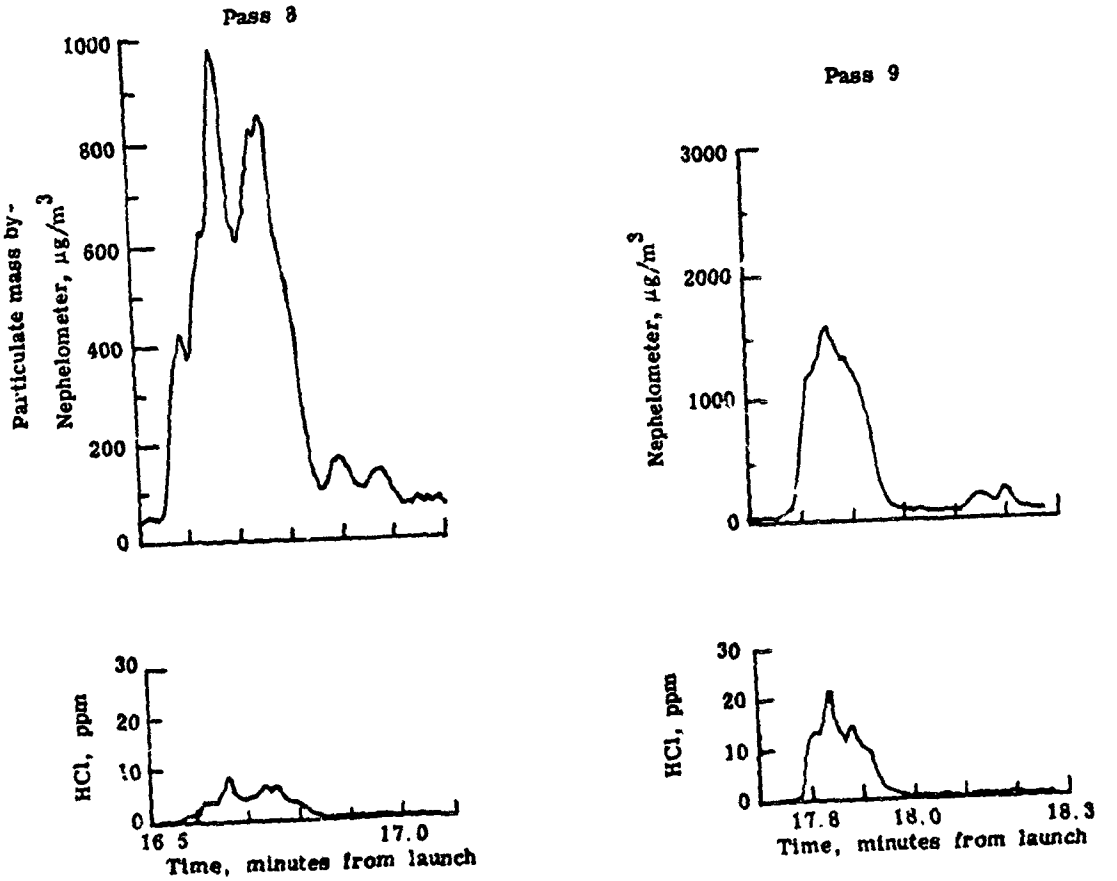

(d) Passes 8 and 9.

Figure 10.- Continued.

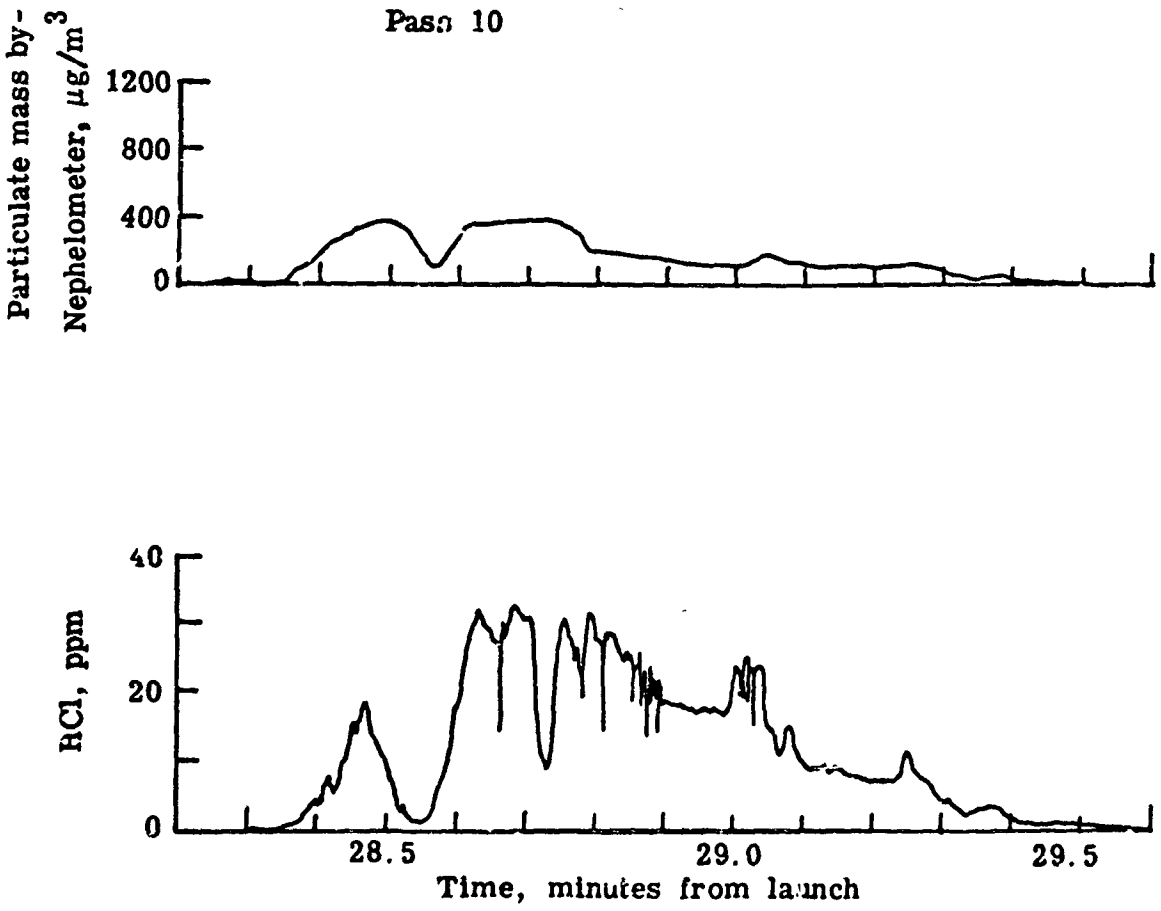

(e) Pass 10.

Figure 10.- Continued.

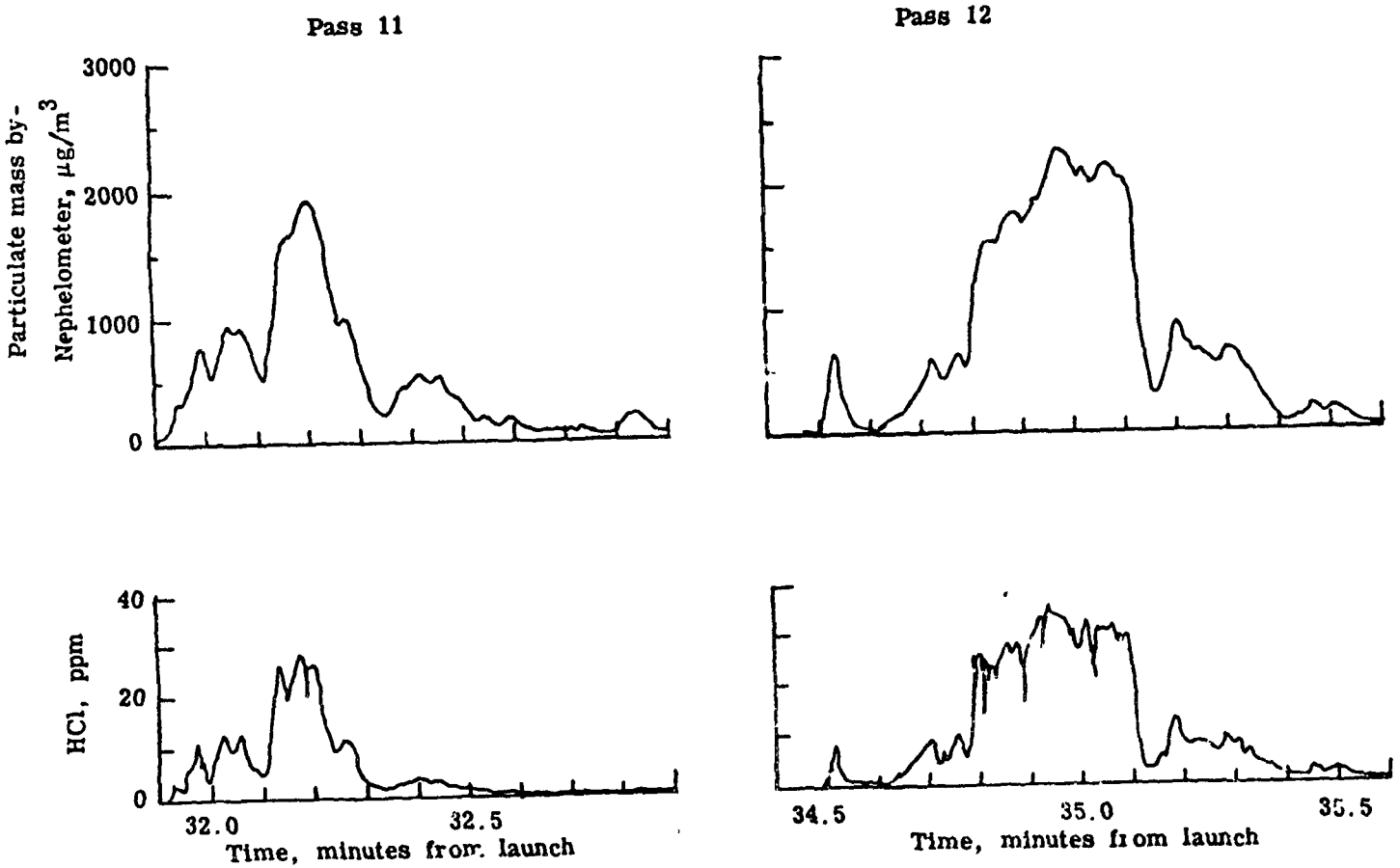

(f) Passes 11 and 12.

Figure 10.- Continued.

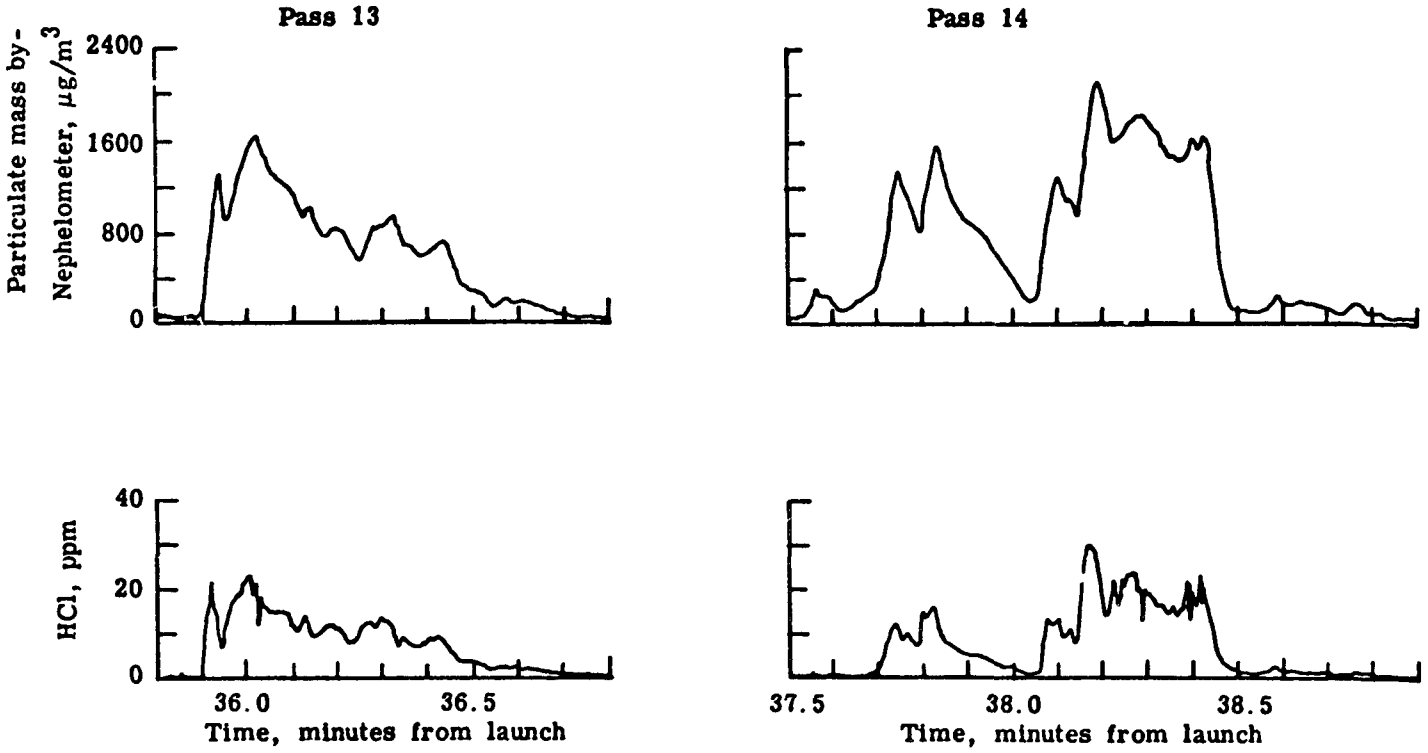

(g) Passes 13 and 14.

Figure 10.- Continued.

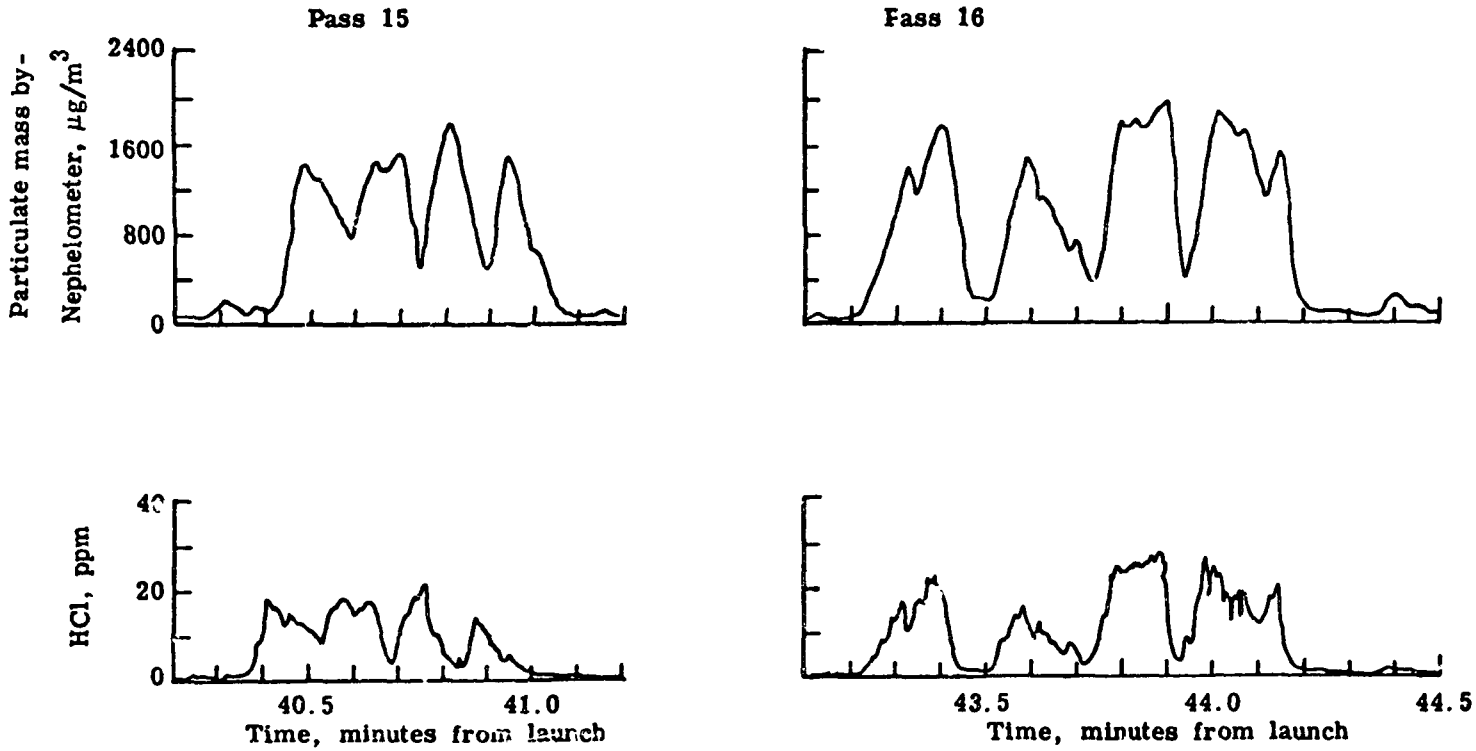

(n) Passes 15 and 16.

Figure 10.- Continued.

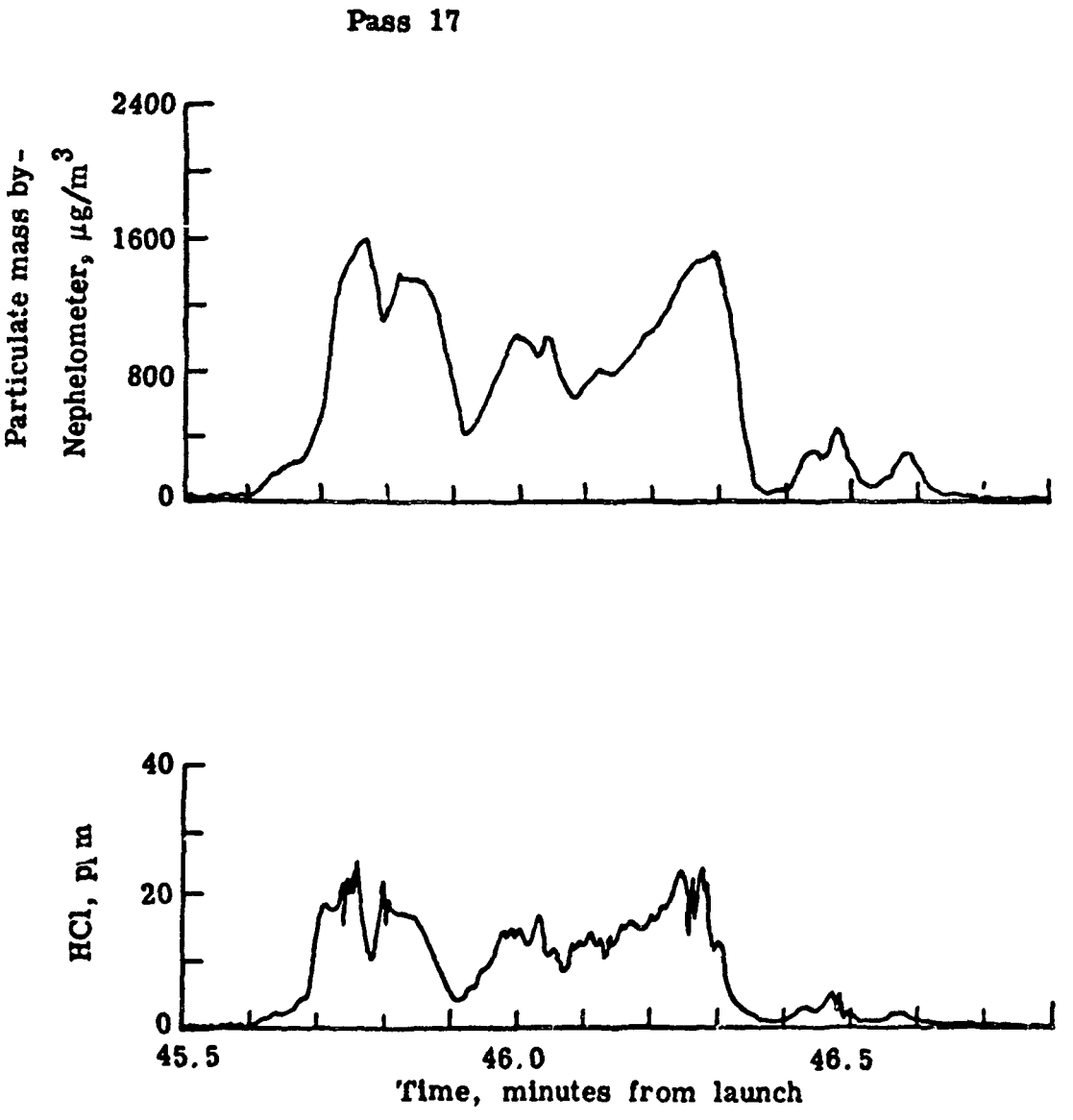

(i) Pass 17.

Figure 10.- Continued.

Pass 18

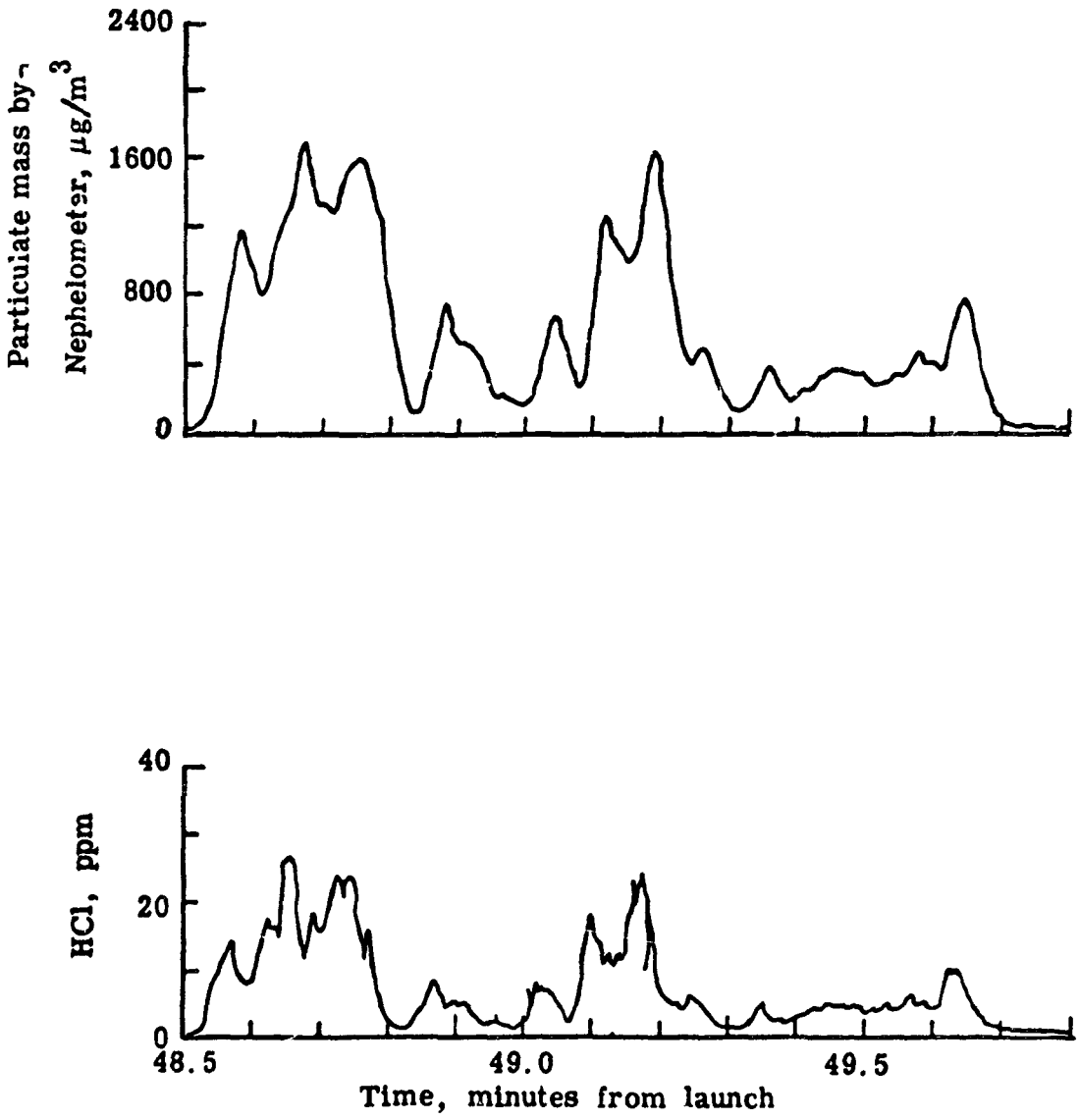

(j) Pass 18.

Figure 10.- Continued.

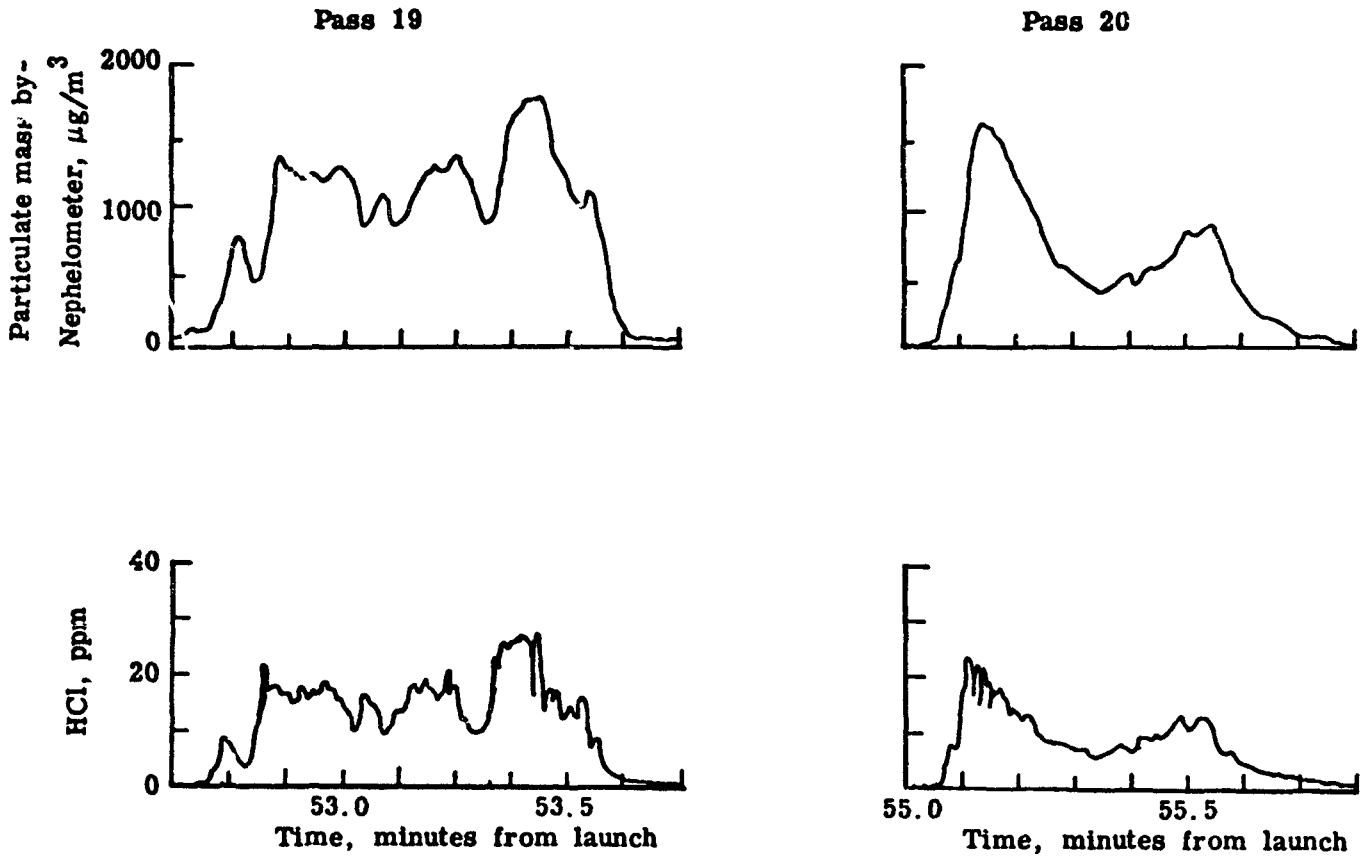

(k) Passes 19 and 20.

Figure 10.- Concluded.

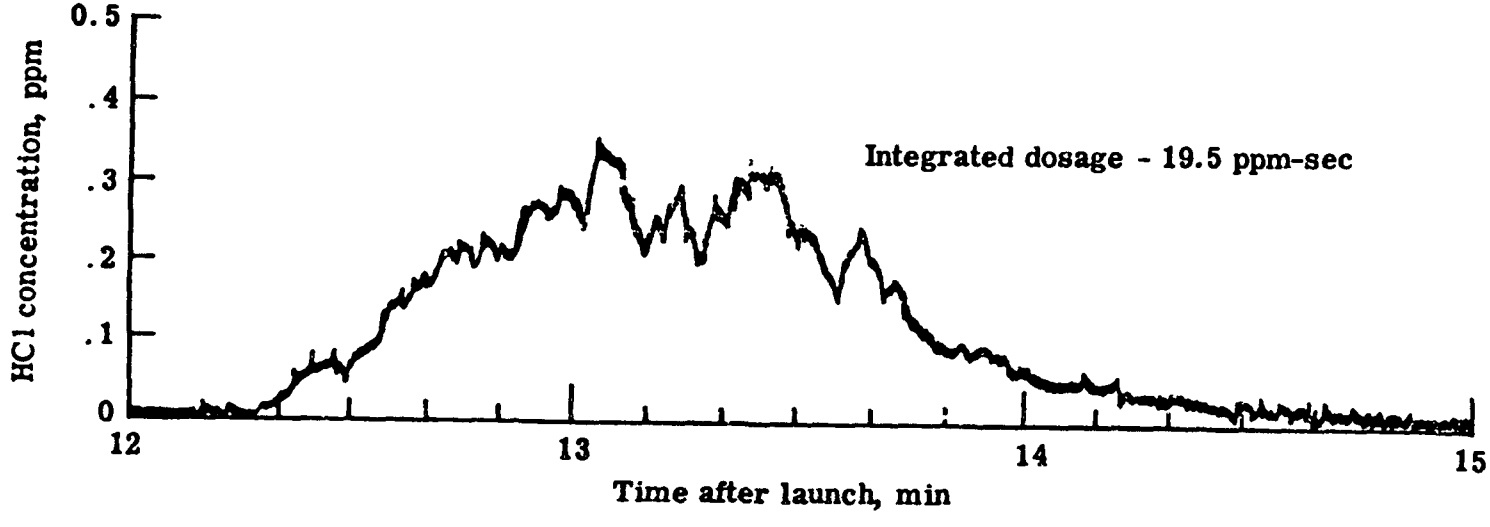

(a) Site P-2.

Figure 11.- Hydrogen chloride surface measurements.

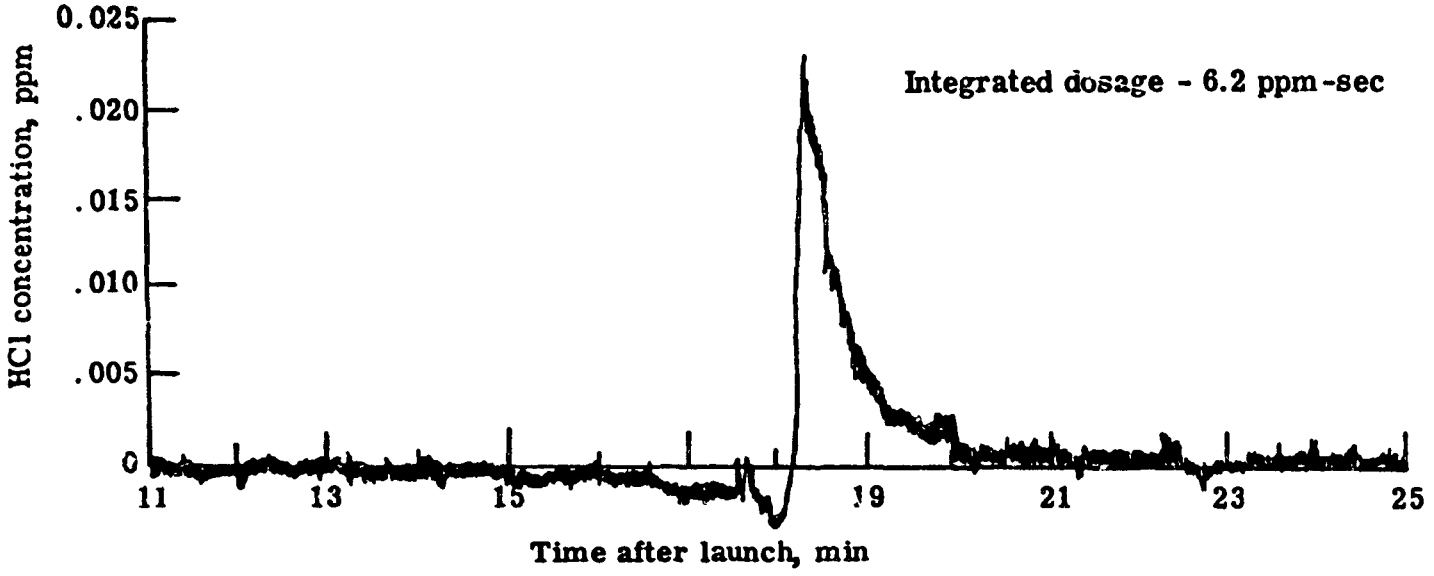

(b) Site P-3.

Figure 11.- Continued.

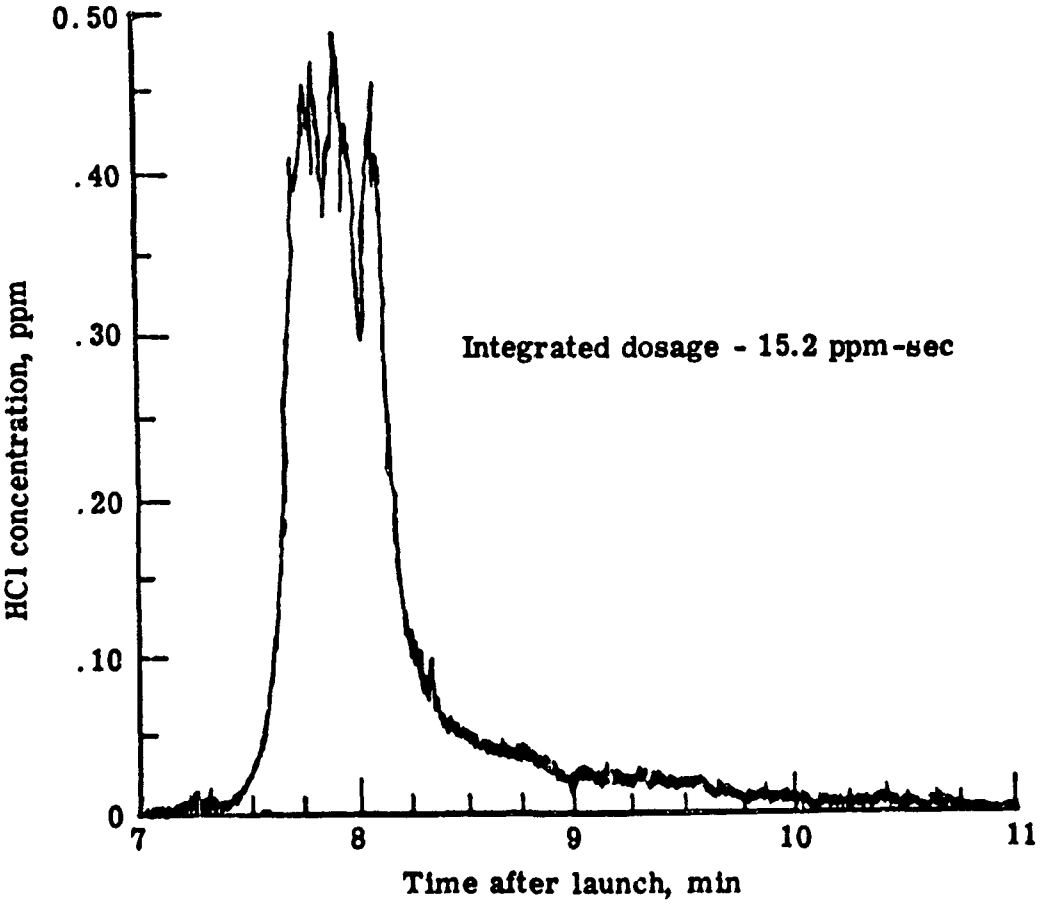

(c) Site P-4.

Figure 11.- Concluded.

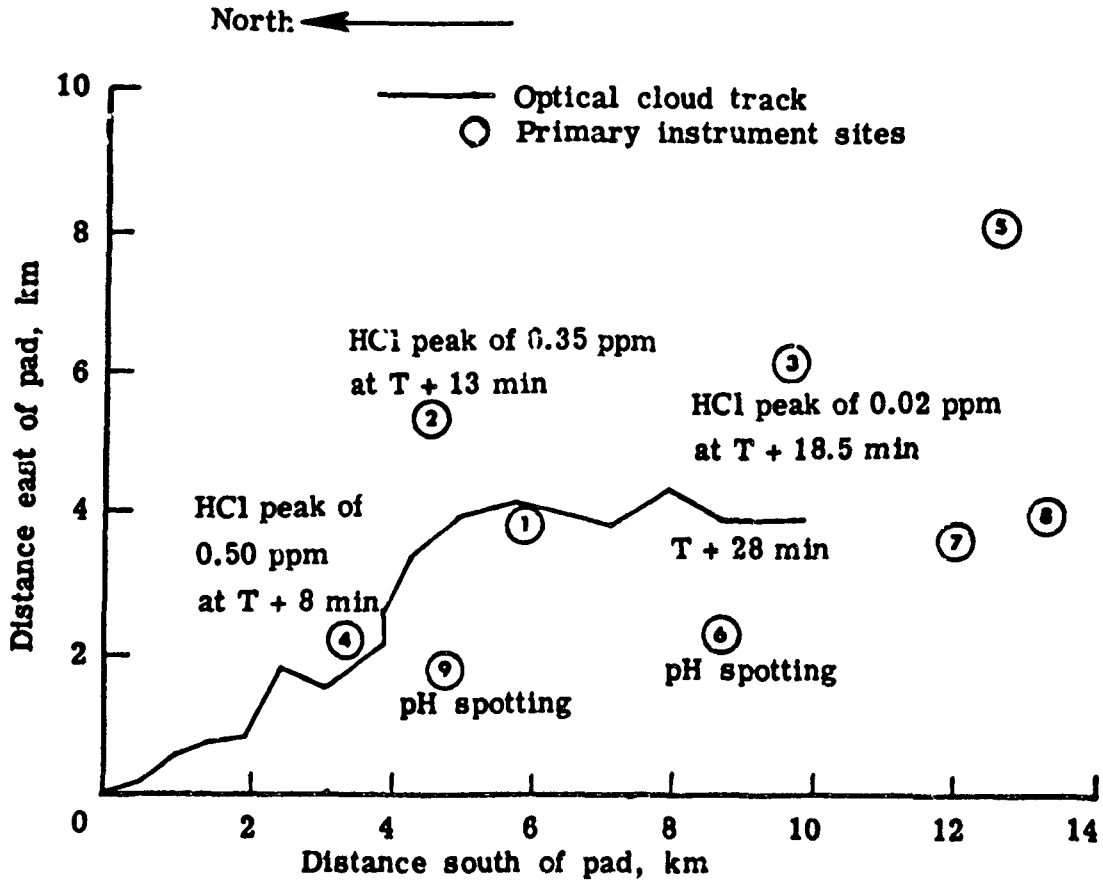

Figure 12.- Surface detection of HCl relative to the optically measured cloud track.